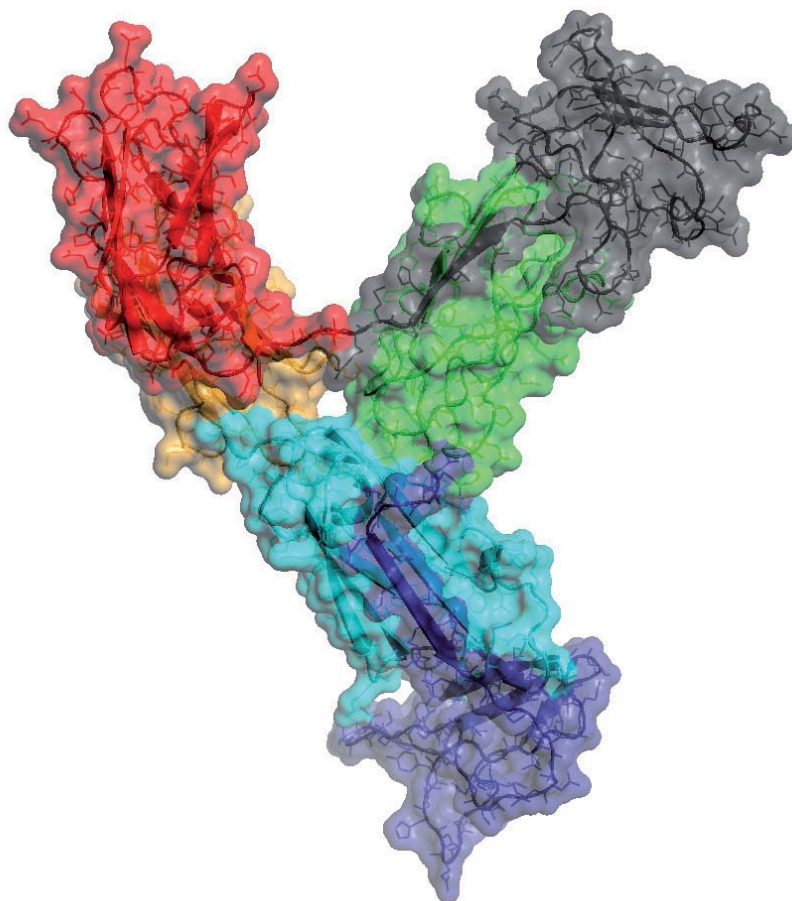Salla Ruskamo

Structures, Interactions and Packing of Filamin Domains

Salla Ruskamo

Structures, Interactions and Packing of Filamin Domains

UNIVERSITY OF JYVÄSKYLÄ

Structures, Interactions and Packing of Filamin Domains

Salla Ruskamo

Structures, Interactions and Packing of Filamin Domains

UNIVERSITY OF JYVÄSKYLÄ

Cover picture: The small-angle X-ray scattering model of filamin A domains 16-21.
Each domain is represented in different colors (16 in orange, 17 red, 18 grey, 19 green,
20 blue and 21 cyan).

"If we did all the things we are capable of,
we would literally astound ourselves. "

-Thomas A. Edison

ABSTRACT

Filamins (FLNs) are actin crosslinkers and scaffolding proteins that participate in multiple cellular processes including cell adhesion, movements, signaling and transcriptional regulation. FLN gene mutations cause several disorders with defects in the brain as well as in the skeletal and cardiovascular systems. Human FLNs are large dimers composed of an N terminal actin-binding domain (ABD) and 24 immunoglobulin-like domains that are divided into rod 1 and rod 2 regions by a flexible hinge 1 segment. Domains 1-15 form rod 1, and rod 2 includes domains 16-24. In this thesis, the crystal structure of the filamin A (FLNa) ABD was solved. It revealed a conserved helical fold with two calponin homology domains connected by a linker. The exact location of patient mutations in ABD was specified, and their effects on the conformation and actin-binding properties of ABD were considered. In addition, the crystal structure of FLNa domain 21-migfilin complex was solved. The atomic details showed a similar binding mode as in previous FLN complex structures, suggesting the common interaction pattern of FLN Ig-like domains. Most FLN binding partners interact with the C terminal rod 2 region. In this thesis, we show evidence of two novel and one previously known closely packed domain pairs in this region. In two of the domain pairs, the major ligand binding site is masked between the domains, whereas in one of the pairs the ligand binding site is accessible for interactions. We further studied the low-resolution structure of the six-domain fragment containing these three domain pairs and found that they form a compact, three-branched structure. This structure was shown to be markedly altered by binding of ligand peptides to the masked interaction sites. This provides a mechanism to regulate FLN interactions and supports the role of FLN as a mechanosensor, because the same conformational changes could take place upon mechanical stretching of FLN and thus regulate the binding of regulatory proteins.

Keywords: actin-binding domain, filamin, immunoglobulin-like domain, integrin, migfilin

Salla Ruskamo, University of Jyväskylä, Division of Cell and Molecular Biology, Department of Biological and Environmental Sciences, P.O. Box 35, FI-40014 University of Jyväskylä, Finland

Author's address   Salla Ruskamo
Department of Biological and Environmental Science
P.O. Box 35
FI-40014 University of Jyväskylä
Finland
salla.ruskamo@jyu.fi

Supervisor   Professor Jari Ylänne, Ph.D.
Department of Biological and Environmental Science
P.O. Box 35
FI-40014 University of Jyväskylä
Finland

Reviewers   Docent Pirta Hotulainen, Ph.D.
Neuroscience Center
P.O. Box 56
FI-00014 University of Helsinki
Finland

Docent Tiina Salminen, Ph.D.
Department of Biochemistry and Pharmacy
Åbo Akademi University
Tykistökatu 6A
FI-20520 Turku
Finland

Opponent   Docent Petri Kursula, Ph.D.
Department of Biochemistry
P.O. Box 3000
FI-90014 University of Oulu
Finland

CONTENTS

ABSTRACT
CONTENTS
LIST OF ORGINAL PUBLICATIONS
RESPONSIBILITIES OF SALLA RUSKAMO IN THE THESIS ARTICLES
ABBREVIATIONS

Acknowledgements
YHTEENVETO (RÉSUMÉ IN FINNISH)
REFERENCES

LIST OF ORGINAL PUBLICATIONS

This thesis is based on the following original publications, which will be referred to in the text by their Roman numerals.

I   Ruskamo, S. & Ylänne, J. 2009. Structure of the human filamin A actin-binding domain. Acta Crystallogr.D Biol.Crystallogr. 65:1217-1221.

II   Lad, Y.,* Jiang, P.,* Ruskamo, S.,* Harburger, D.S., Ylänne, J., Campbell, I.D. & Calderwood, D.A. 2008. Structural basis of the migfilin-filamin interaction and competition with integrin beta tails. J.Biol.Chem. 283:35154-35163.

III   Heikkinen, O.K., Ruskamo, S., Konarev, P.V., Svergun, D.I., Iivanainen, T., Heikkinen, S.M., Permi, P., Koskela, H., Kilpeläinen, I. & Ylänne, J. 2009. Atomic structures of two novel immunoglobulin-like domain pairs in the actin cross-linking protein filamin. J.Biol.Chem. 284: 25450-25458.

IV   Ruskamo, S., Ylänne, J. & Pentikäinen U. Filamin domain assembly regulates its C terminal interactions: Structure and flexibility of six domain fragment. Manuscript.

*Equal contribution

RESPONSIBILITIES OF SALLA RUSKAMO IN THE THESIS ARTICLES

Article I   I conducted all experimental work including DNA cloning, protein expression, purification and crystallization. I collected the diffraction data together with Jari Ylänne. I processed the data and solved and refined the structure. The authors planned and wrote the article together. I prepared all the figures.

Article II   I expressed and purified the protein for the crystallization assays and crystallized the protein-peptide complex. I collected the diffraction data together with Jari Ylänne, and I conducted data processing, structure solution and refinement. I analyzed the final structure. I participated in writing the article and preparing the figures.

Article III I cloned the DNA constructs and expressed and purified the proteins with help from Kati Viitaniemi and Arja Mansikkaviita. Together with Peter Konarev and Jari Ylänne, I measured the small-angle X-ray scattering data. I also analyzed the data and built *ab initio* models in collaboration with Peter Konarev. I performed the pull-down binding assays and participated in planning and writing the article and preparing the figures.

Article IV   I conducted the DNA cloning and mainly all protein expression and purification. Emilia Horttana performed the mutagenesis. Together with Ulla Pentikäinen, I measured the small-angle X-ray scattering data. I did all the small-angle X-ray scattering data analysis as well as the *ab initio* and rigid-body modeling. I planned and wrote the manuscript together with Ulla Pentikäinen and Jari Ylänne. I prepared the figures.

All the studies in this thesis were performed under the supervision of Professor Jari Ylänne.

ABBREVIATIONS

ABD   actin-binding domain
ABS   actin-binding site
CH   calponin homology
D_{max} maximum linear dimension
DR   dopamine receptor
ECM   extracellular matrix
F-actin   filamentous actin
FilGAP   filamin A-binding RhoGTPase activating protein
FLN   filamin
FLNa   filamin A
FLNb   filamin B
FLNc   filamin C
GPIbα   glycoprotein Ibα
GTPase   guanosine triphosphatase
Ig   immunoglobulin
LIM   Lin-11, Isl-1, Mec-3
NMR   nuclear magnetic resonance
OPD   otopalatodigital
PEBP2/CBFβ   polyomavirus enhancer binding protein 2/core binding factor β
PVNH   periventricular nodular heterotopia
R_g radius of gyration
rmsd   root mean square deviation
SAXS   small-angle X-ray scattering
SDS-PAGE   sodium dodecyl sulfate polyacrylamide gel electrophoresis
VASP   vasodilator-stimulated phosphoprotein

1   INTRODUCTION

The actin cytoskeleton has multiple functions in cells. It maintains the cell shape but also participates in several vital cellular processes including, cell adhesion, cell movement and formation of different types of cell extensions. The actin cytoskeleton is a dynamic network of actin filaments that is regulated and modulated by several actin-binding and signaling proteins. One of these protein families is called filamins (FLNs). FLNs crosslink actin filaments and thus participate in numerous actin cytoskeleton-related cellular processes. FLNs are, however, much more than only cytoskeletal structural units as they serve as scaffolds for signaling proteins, are essential components of cell-cell and cell-extracellular matrix (ECM) adhesion sites and even participate in transcriptional regulation in the nucleus (Zhou et al. 2010). The development of the brain, skeleton and cardiovascular system requires the proper FLN expression in cells, and thus several FLN gene-mutation-causing disorders have been discovered.

This doctoral thesis focuses on the structural properties and interactions of filamin A (FLNa). The atomic structures of FLNa actin-binding domain (ABD) (I) as well as the complex structure of FLNa immunoglobulin (Ig)-like domain 21 and the migfilin peptide were solved (II). In addition, the overall structure and domain arrangement of the C terminal region of FLNa was investigated (III, IV). Ligand binding was shown to cause remarkable structural changes in this region (IV).

Detailed structural information about FLNs is required for understanding their interactions and function. This information may also provide a new insight into the molecular-level effects of human disorders causing FLN mutations (Feng & Walsh 2004).

2 REVIEW OF THE LITERATURE

2.1 Actin-binding proteins

The actin cytoskeleton is a filament network capable of remodeling the cell morphology and responding to environmental changes or changes in cell differentiation status. Although the actin filament itself has some striking dynamic features, all actin cytoskeleton functions are regulated by various actin-binding proteins (Revenu et al. 2004, Lee & Dominguez 2010). Actin crosslinkers are a subgroup of actin-binding proteins that are specialized to link actin filaments (F-actin) to form bundles or three-dimensional networks. This group includes multiple proteins, such as α-actinins, spectrins, plectins, dystrophins, fimbrins and FLNs, that all share a conserved ABD (Gimona et al. 2002).

2.2 Filamins

Filamins are large and flexible actin-binding proteins that link actin filaments together with a broad distribution of angles (Revenu et al. 2004). The FLN protein family is distributed over the animal kingdom. Humans and other vertebrates have three FLN genes, *FLNA*, *FLNB* and *FLNC*, that are highly conserved with a sequence identity of about 64 %. Several mRNA splice variants of these isoforms are also known. In addition to vertebrates, FLNs have also been discovered in the *Drosophila melanogaster* fruit fly (Sokol & Cooley 1999), *Caenorhabditis elegans* round worm, *Dictyostelium discoideum* slime mold (Hock & Condeelis 1987) and *Entamoeba histolytica* parasite (Vargas et al. 1996). FLNs have not been found in either plants or fungi. The domain composition and length of FLN peptide chains differ from species to species; the FLNs of primitive species often include fewer domains than their mammalian orthologs.

The expression patterns of human FLNs vary in tissues; FLNa is the most ubiquitously expressed (Gorlin et al. 1990), but the filamin B (FLNb) is also found in several cell types (Takafuta et al. 1998). On the contrary, filamin C (FLNc) expression is mostly limited to the skeletal and cardiac muscle tissues (Thompson et al. 2000). All three mammalian FLNs have, however, a crucial role in tissue development and in cell homeostasis. Thereby, mutations in human FLN genes trigger severe genetic disorders, inducing malformations in the brain, the skeleton and the cardiovascular system (Robertson et al. 2003, Krakow et al. 2004, Vorgerd et al. 2005, Kyndt et al. 2007).

2.2.1 The overall structure of filamin A

The human FLNa monomer is a 280 kDa elongated protein composed of an N terminal ABD followed by a relatively long rod region (Fig. 1). This rod consists of 24 Ig-like domains that are divided into rod 1, containing domains 1-15, and rod 2 (domains 16-24) by a flexible, non-conserved, 25-residue-long hinge 1 segment. The other flexible, 35-residue-long hinge segment, hinge 2, is situated between the Ig-like domains 23 and 24 (Gorlin et al. 1990). Based on the electron micrographs, the length of rod 1 is directly comparable with the number of 4.5 nm-long Ig-like domains. The measured average length of rod 1 (~65 nm) is in agreement with the calculated length of 15 Ig-like domains (15 * 4.5 nm = 67.5 nm) but the rod 2 region seems to be more compact, only ~20 nm long, compared to the estimated length of 8 Ig-like domains (8 * 4.5 nm = 36.0 nm) (Nakamura et al. 2007).

To be able to link two actin filaments, FLNa have to comprise two ABDs. In fact, electron microscopy studies show that the biological and functional form of FLNa is a Y- or V-shaped dimer in which the average angle between two FLNa chains is ~80-90° (Gorlin et al. 1990, Nakamura et al. 2007). The dimerization of all FLNs occurs through the most C terminal Ig-like domain (Gorlin et al. 1990, Popowicz et al. 2004, Pudas et al. 2005, Seo et al. 2009).
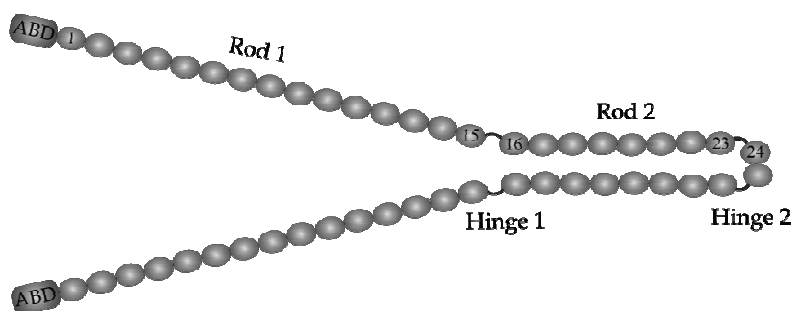

FIGURE 1   A diagram of the overall structure of FLNa. The N terminal ABD (dark grey) is followed by the rod region consisting of 24 Ig-like domains (light grey ellipses). Two hinges increase the flexibility of the rod. The dimerization occurs through domain 24.

12

2.2.1.1 The actin-binding domain

The actin-binding domains of FLNs are composed of ~280 residues. Based on the sequence alignments, human FLN ABDs, similar to all other vertebrate FLN ABDs, comprise two tandem calponin homology (CH) domains connected by a linker region. Each CH domain is ~110 residues long, highly conserved, and forms a helical fold. The domain arrangement, in which the type 1 CH domain is followed by the type 2 CH domain, is common in cytoskeletal F-actin-binding proteins and can be found, for example, in the N terminal part of α-actinins, β-spectrins, plectins, dystrophins and utrophins (Gimona et al. 2002). Two different ABD conformations have been observed in crystal structures. In the closed conformation, CH domains lie in proximity to each other and interact via several salt bridges (Fig. 2A) (Garcia-Alvarez et al. 2003, Borrego-Diaz et al. 2006). In open conformation, the two CH domains of one molecule are distant (Fig. 2B) but interact with the CH domains of the neighboring molecule, forming the similar domain-domain interface as in the closed structure. This open arrangement in the crystal lattice can also be called a domain swap between two polypeptides (Keep et al. 1999). There are some indications that the flexible nature of ABDs that is manifested in the domain swap also has a role in their interactions with F-actin (Galkin et al. 2002, Liu et al. 2004).

In most ABDs, there are multiple actin-binding sites (ABSs), two in CH1 and one in CH2. Typically, a single CH2 domain is not capable of interacting with F-actin while the CH1 domain alone binds to F-actin but with 10-fold lower than the whole ABD (Banuelos et al. 1998). The actual interaction and regulation mechanisms of actin binding of FLN ABDs are still unknown. However, a Ca^{2+}-binding protein, calmodulin, inhibits FLNa binding to F-actin and actin gelation performed by FLNa. Intriguingly, Ca^{2+}-calmodulin does not bind to full-length FLNa in the absence of actin but binds to denatured FLNa ABD. This action suggests that some conformational change on FLNa ABD takes place due to actin binding and exposes the Ca^{2+}-calmodulin binding site (Nakamura et al. 2005).
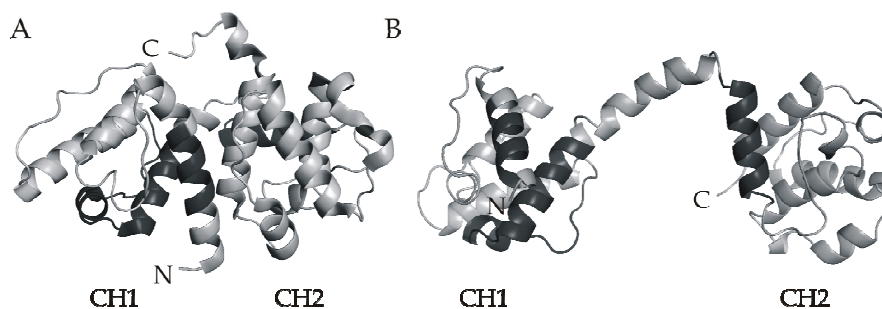
FIGURE 2   A. The crystal structure of α-actinin 1 ABD in the closed conformation (PDB code 2EYI, Borrego-Diaz et al. 2006). ABSs are represented in black. B. The crystal structure of utrophin ABD in the open conformation (1QAG, Galkin et al. 2002).

2.2.1.2 Filamin immunoglobulin-like domains

All Ig-like domains in human FLNs, excluding FLNc20, are ~100 resides long (van der Flier & Sonnenberg 2001) and the diameters of the domains are approximately 4.5 nm x 2.5 nm x 1.7 nm. They are generally composed of seven (A-G) 6-10 residues long, β strands that are connected by loops and form two antiparallel β sheets. The β strands A, B, E and D form one sheet of the fold, and C, F and G lie in the other sheet (Fig. 3). These β sandwich folds belong to the E subtype of the Ig family (Pudas et al. 2005). Nowadays, there are plenty of structures of single FLN domains available, and the Ig-like fold seems to be rather conserved. However, the single-domain structures of FLNc16 (PDB code 2D7F), FLNb18 (2DMC) and FLNb20 (2DLG) show that the first (A) strands of these Ig-like domains have not been folded together with the rest of the domain but are detached and unstructured.
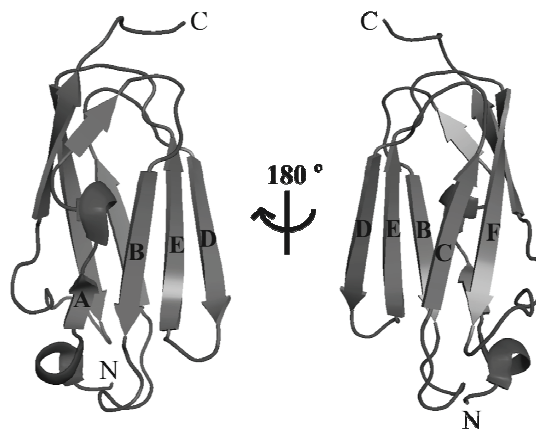
FIGURE 3   The crystal structure of FLNc23 (PDB code 2NQC, Sjekloca et al. 2007) represented as a cartoon from two different angles. The typical FLN Ig-like domain contains seven β strands (A-G) that form two β sheets.

2.2.1.3 The domain pair of filamin A domains 20 and 21

The crystal structure of FLNa domains 19-21 reveals the unforeseen co-operative folding of Ig-like domains (Lad et al. 2007). In the structure, FLNa19 and 21 are folded as typical Ig-like domains, but FLNa20 is partially unfolded while its A strand interacts with the CD face of FLNa21 forming a domain pair. In this domain pair, FLNa20 is situated crosswise at the end of FLNa21, and several interactions are formed between FLNa20 G strand and the BC loop of FLNa21. The binding site of the FLNa20 A strand in FLNa21 is the same as the known integrin binding site. In accordance with this, the presence of FLNa20 was shown to decrease the integrin-binding affinity compared to FLNa21 alone

(Lad et al. 2007). Thus, integrin binding to FLNa21 is partially auto-inhibited by the neighboring domain.

2.2.2 Interaction partners of filamin A rod 2 region

The FLNa rod 2 region, containing Ig-like domains 16-24, interacts with more than 50 proteins, including transmembrane receptors, cytoplasmic adapter and signaling proteins as well as transcription factors. In addition, both full-length FLNa and a C terminal 90-100 kDa FLNa fragment have been observed to co-localize with some nuclear proteins in nucleus (Ozanne et al. 2000, Loy et al. 2003, Berry et al. 2005).

The interaction modes of some FLN Ig-like domains and their binding partners have been determined (Kiema et al. 2006, Nakamura et al. 2006, Nakamura et al. 2009). Those structures reveal that the interaction usually takes place through the face that is composed of the C and D strands, thus termed the CD face. The dimerization of vertebrate FLNs also occurs via the CD face of the last Ig-like domain (Pudas et al. 2005, Seo et al. 2009). FLNa rod 2 region binding partners are listed in Table 1. The interaction partners that are most relevant to this work are described in more detail in the following chapters.

TABLE 1 FLNa rod 2 interaction partners

Protein	Interaction domain	Reference
Receptors and ion channels		
Calcium sensing receptor	14-16	(Awata et al. 2001)
Dopamine receptors D2, D3 (DR D2, DR D3)	16-19	(Li et al. 2000, Li et al. 2002)
Glycoprotein Ibα (GPIbα)	17	(Nakamura et al. 2006)
G protein coupled calcitonin receptor	20-21	(Seck et al. 2003)
Insulin receptor	22-24	(He et al. 2003)
Integrins β1, β2, β2, β3, β7	21, 19	(Loo et al. 1998)
Metabotrobic glutamate receptor type 7	21-22	(Enz & Croci 2003)
Hyperpolarization-activated, cation nonselective pacemaker channel 1 (HCN1)	23-24	(Gravante et al. 2004)
Voltage-gated K$^+$ channel 4.2 (Kv4.2), Rectifying K$^+$ channel 2.1 (Kir2.1)	20-24	(Petrecca et al. 2000, Sampson et al. 2003)
Presenilin 1, 2	22-24	(Zhang et al. 1998)
Tissue factor	24	(Ott et al. 1998)
µ opioid receptor	Hinge2-24	(Onoprishvili et al. 2003)
Cystic fibrosis transmembrane conductance regulator (CFTR)	9, 12, 17, 19, 21, 23	(Playford et al. 2010)
Carcinoembryonic antigen-related cell adhesion molecule 1 (CEACAM1)	23-24	(Klaile et al. 2005)

(continues)

TABLE 1 (continues)

Signaling proteins, kinases and phosphatases		
Filamin A-binding RhoGTPase activating protein (FilGAP)	23	(Nakamura et al. 2009)
Mitogen-activated protein kinase kinase 4 (MKK4)	21-23	(Marti et al. 1997)
Mitogen-activated protein kinase kinase 7γ2 (MKK7γ2)	22-24	(Nakagawa et al. 2010)
p21-activated kinase (Pak-1)	23	(Vadlamudi et al. 2002)
Protein kinase Cα (PKCα)	1-4, Hinge2-24	(Tigges et al. 2003)
ROCK	24	(Ueda et al. 2003)
SH2-domain-containing inositol 5'-phosphatase 2 (SHIP-2)	22-24	(Dyson et al. 2001)
Smad2, 4, 5, 6	20-24	(Sasaki et al. 2001)
RhoA, Rac1, CDC42, Ra1A	24	(Ohta et al. 1999)
Sphingosine kinase 1 (SphK-1)	15-16, 19-21	(Maceyka et al. 2008)
Trio	23-24	(Bellanger et al. 2000)
Adaptor proteins		
Focal adhesion protein 52 (FAP52)	14-16	(Nikki et al. 2002)
Filamin *A*-interacting protein (FILIP)	15-18	(Nagano et al. 2002)
Pleckstrin homology-like domain, family B, member 2 (PHLDB2)/LL5β	22-24	(Takabayashi et al. 2010)
Migfilin	21	(Tu et al. 2003)
Truncated c-maf inducing protein (Tc-mip)	16-17	(Grimbert et al. 2004)
Nuclear proteins		
Androgen receptor	16-19	(Ozanne et al. 2000)
Forkhead box protein C1 (FOXC1)	4-5, 6-9, 16-21	(Berry et al. 2005)
Polyomavirus enhancer binding protein 2/core binding factor β (PEBP2/CBFβ)	23-24	(Yoshida et al. 2005)
Others		
Caveolin-1	22-Hinge2	(Stahlhut and van Deurs 2000)
cv heat shock protein (cvHsp)	23-24	(Krief et al. 1999)
Endothelial cell–specific molecule-2 (ECSM-2)	15-16, 19-21	(Armstrong et al. 2008)
Granzyme B	20-24	(Browne et al. 2000)
Nephrocystin	15-16	(Donaldson et al. 2002)
Pro-prion	10, 16, 17, 18, 20, 21, 23	(Li et al. 2010)
Prostate specific membrane antigen (PMSA)	23-24	(Anilkumar et al. 2003)
Breast cancer associated protein 2 (BRCA-2)	21-24	(Yuan & Shen 2001)
Epithin	14-24	(Kim et al. 2005)

2.2.2.1 Integrins

Integrins are a family of transmembrane adhesion receptors that provide a linkage between the actin cytoskeleton and the ECM. They are heterodimers composed of non-covalently associated α and β subunits (Fig. 4). In total, 18 α and 8 β subunits exist forming 24 different heterodimers that all consist of a large ectodomain, a helical transmembrane region and relatively short cytoplasmic tails (Hynes 2002). Integrin conformation changes from "bent" to "extended" according to the activity level that is regulated by multiple cellular proteins (Xiong et al. 2001, Takagi et al. 2002, Nishida et al. 2006). Integrins are a crucial component of cell-ECM adhesions and contribute to cellular signaling to regulate cell migration, proliferation, differentiation and survival. Therefore, integrins participate in several processes in tissues, including morphogenesis, wound healing and metastasis (Gahmberg et al. 2009).
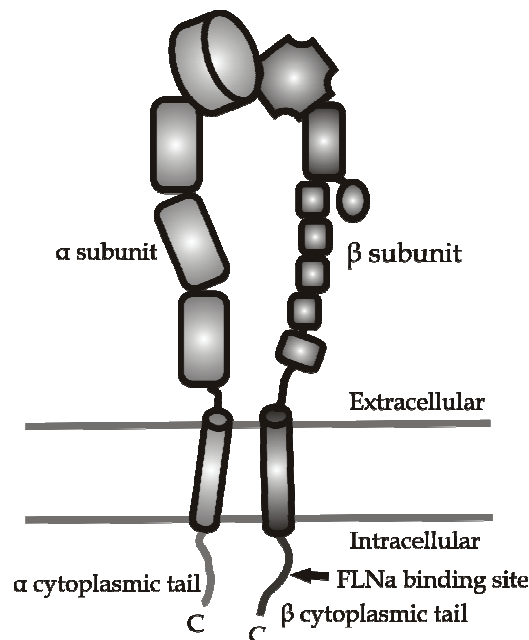
FIGURE 4   The schematic view of the extended form of integrin generated based on the molecular model of αVβ3 integrin (Xiong et al. 2001). α subunit is represented in light grey and β subunit in dark grey. The FLNa binding site in the β cytoplasmic tail is pointed by the arrow.

Filamin A is a piece of the complex integrin regulation puzzle. FLNa binds to the cytoplasmic tails of the integrin β subunits and links them to the actin cytoskeleton (Calderwood et al. 2001). Both Ig-like domains 19 and 21 interact with integrin, but FLNa21 has a higher binding affinity and is, therefore, the primary binding site of integrins (Kiema et al. 2006, Takala et al. 2008). As mentioned earlier, the binding site is masked by the first strand of FLNa20, suggesting some auto-inhibition in integrin binding (Lad et al. 2007). The FLNa binding site in integrins overlaps with the binding site of talin, the most

important integrin activator. Talin and FLNa compete for the integrin binding, and FLNa binding to integrin thus affects the talin-induced integrin activation. In FLNa deficient cells, integrins have also been observed to be more active while talin binding has not been inhibited by FLNa (Kiema et al. 2006).

2.2.2.2 Migfilin

Migfilin, also called filamin-binding LIM protein-1, is a ~50 kDa FLN interacting protein that has a role in cell shape modulation (Takafuta et al. 2003). It is widely expressed in human tissues, and it is composed of three C terminal LIM (Lin-11, Isl-1, Mec-3) domains, a central proline-rich region and an N terminal region that, based on sequence comparisons, do not contain any previously known protein folds (Fig. 5). One migfilin mRNA splice variant, migfilin (s), which lacks the central proline-rich region, has been found in several different cell types simultaneously with the full-length migfilin (Tu et al. 2003).

Based on the first studies, migfilin was found to localize to cell-ECM adhesion sites and to actin stress fibers. The association with F-actin occurs through FLNa and FLNb (Tu et al. 2003, Takafuta et al. 2003). The localization in cell-ECM adhesion sites is mediated by kindlin-2 (mig-2) that binds to two of the most C terminal LIM domains of migfilin (Fig. 5) (Tu et al. 2003). Kindlin-2 is an essential protein that interacts directly with the integrin β tails and serves as an integrin co-activator (Ma et al. 2008, Harburger et al. 2009).

Migfilin also interacts with vasodilator-stimulated phosphoprotein (VASP) through its central proline-rich region (Fig. 5). The exact VASP binding site in migfilin has been mapped on the LPPPPP sequence located in residues 104-109. Migfilin plays a consequential role in localizing VASP in the cell-ECM adhesion sites but not to the lamellipodia. It participates in the regulation of cell motility and is thus required for proper cell migration. The loss of migfilin reduces cell migration but, surprisingly, overexpression has similar effect (Zhang et al. 2006). Migfilin is evidently a key regulator, with a dual role, of cell migration and cell shape modulation.

FIGURE 5   The schematic view of migfilin containing the N terminal part (dark grey), central proline-rich region (light grey) and three C terminal LIM domains (black) (Tu et al. 2003). The Zn^{2+} ions of LIM domains are represented as small circles. The binding sites of migfilin interaction partners FLNa, VASP and Kindlin-2 are also shown.

Migfilin is also a component of different types of cell adhesion sites. It is recruited to cell-cell junctions in epithelial and endothelial cells together with the known cell-cell junction proteins, β catenin and E cadherin. The two most C terminal LIM domains mediate its localization to cell-cell junctions, suggesting

that the binding sites that control the distribution of migfilin to cell-ECM and cell-cell junctions at least partially overlap. Depletion of migfilin inhibits the proper formation of cell-cell junctions and causes the diffuse distribution of β catenin and E cadherin in cells and disorganization of actin filaments (Gkretsi et al. 2005). Accordingly, migfilin links cell-cell and cell-ECM adhesions to the actin cytoskeleton and has an essential role as an adapter protein in cellular adhesions.

2.2.2.3 Dopamine receptors

Dopamine receptors (DRs) are G protein-coupled transmembrane receptors that are targets of the predominant catecholamine neurotransmitter, dopamine. They participate in and regulate several central nervous system functions, including memory, learning and cognition. Thus, they are involved in multiple pathological disturbances such as schizophrenia, Parkinson's disease, drug addiction and attention-deficit hyperactivity disorder (ADHD), which made DRs targets of intensive drug design for the past few decades. In addition to the brain, DRs also exist in the adrenal gland, heart, kidney and blood vessels (Missale et al. 1998, Vallone et al. 2000, Dalley & Everitt 2009).
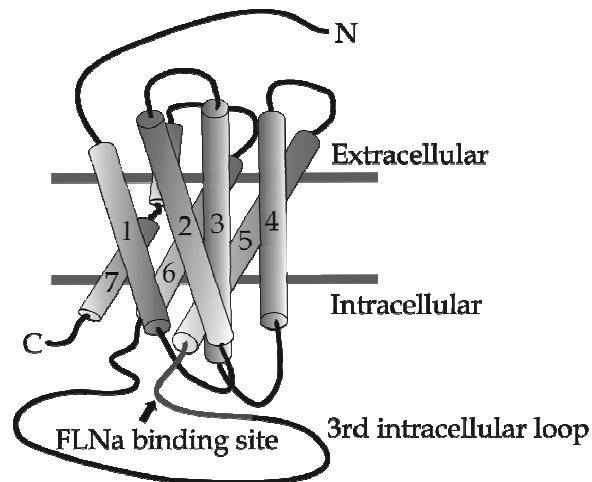
FIGURE 6 The schematic view of DR D3 generated based on the molecular model of DR D3 (Westrich et al. 2010). Seven transmembrane helices are numbered and represented as cylinders. The FLNa binding site (pointed by the arrow) in DR D3 is located in the third intracellular loop.

Dopamine receptors are divided into two subgroups: D1 type receptors, which include D1 and D5 receptors, and D2 type receptors, which are composed of D2, D3 and D4 receptors. All DRs have seven transmembrane helices with an extracellular N terminus and a cytoplasmic C terminus (Fig. 6). The conserved helices are connected by rather short loops. The longest and most divergent loop is the third intracellular loop that also differs in two D2 mRNA splice variants (Vallone et al. 2000).

Dopamine receptor D2 and D3 subtypes, but not D1, D4 or D5 receptors, interact with FLNa in various cell types. The interaction site in the DR is in the third intracellular loop that has been reported to bind to FLNa Ig-like domain 19 (Fig. 6) (Li et al. 2000, Lin et al. 2001, Li et al. 2002). The DR D2/D3-FLNa interaction is crucial for proper DR localization in the plasma membrane together with G proteins (Lin et al. 2001, Lin et al. 2002). The sequestration of DR D3 from the plasma membrane is also FLNa dependent and thus increases the essential role of FLNa in DRs' function (Cho et al. 2007). In addition to proper locating of DRs, FLNa forms a signaling complex with DR D3 and β arrestin. The destabilization of this complex directly alters the signaling potential of DR D3 (Kim et al. 2005).

2.2.3 Functions of filamin A

Filamin A is a component of the complex actin cytoskeleton remodeling system that is composed of multiple actin-binding proteins. FLNa also acts as a scaffold for numerous proteins, improving their ability to signal, and connects the actin cytoskeleton to transmembrane receptors and cell junctions (Stossel et al. 2001). FLNa has a special role in some cellular processes presented here.

2.2.3.1 Filamin A in cell spreading and migration

Filamin A is involved and crucial in the early steps of cell migration in several tissues although other FLNs, FLNb and FLNc, can, at least to some extent, compensate for FLNa deficiency (Kim et al. 2008, Baldassarre et al. 2009). Depletion of FLNa reduces cell spreading and survival, and the number of cell extensions is decreased (Kim et al. 2008). FLNa interacts with collagen-binding β1 integrin that is essential for cell migration (Loo et al. 1998). However, the tight interaction between FLNa and cytoplasmic tails of β integrins reduces cell migration because the formation of transient cell extensions has been inhibited (Calderwood et al. 2001). FLNa regulates the expression of β1 integrins on the cell surface and affects the activation of these integrins together with the intermediate filament protein, vimentin. It associates directly with vimentin and induces the protein kinase C mediated phosphorylation of vimentin that leads to β1 integrin recycling to the plasma membrane (Kim et al. 2010a, Kim et al. 2010b). Thus, FLNa is required for efficient cell migration, but the equilibrium in integrin-FLNa interaction is necessary while inappropriate binding impairs cell migration. However, the exact role of FLNa in cell migration is still unclear, and several contradictory findings have been obtained.

Filamin A affects cell motility also by serving as the scaffold for multiple small guanosine triphosphatases (GTPases) of the Rho family (RA1A, RhoA, Rac and Cdc42) (Ohta et al. 1999) and their upstream and downstream regulators, including the p21 activated kinase-1 (Vadlamudi et al. 2002), ROCK (Ueda et al. 2003), Trio (Bellanger et al. 2000) and filamin A-binding RhoGTPase activating protein (FilGAP) (Ohta et al. 2006). Rho family GTPases regulate actin

assembly and thus influence the formation of cell extensions and regulate cell migration. Many of these signaling proteins bind to FLNa Ig-like domains 23 or 24 and co-localize with FLNa in actin structures (Bellanger et al. 2000, Ueda et al. 2003, Nakamura et al. 2009). Consequently, FLNa mutations trigger several human disorders that may be caused by improper cell adhesion or migration in tissues.

2.2.3.2 Filamin A as a mechanosensor

Cells grow in a mechanically active environment, and they are exposed to high-amplitude tensile forces. Even then, cells have to maintain the cell shape, adhesions and membrane integrity. Cells are able to reinforce the mechanical forces by locally inducing actin accumulation and assembly and recruiting FLNa into cortical adhesion sites (Glogauer et al. 1998). The increase in the levels of other adhesion site proteins, such as integrins or vinculin, has not been observed (Glogauer et al. 1998). The force-induced FLNa enrichment in the adhesion sites is regulated by phosphorylation of FLNa by protein kinase C (Glogauer et al. 1998). FLNa expression also increases in cells that are exposed to $\beta 1$ integrin mediated tensile forces due to the longer half-life of FLNa mRNA and the activation of the *FLNA* gene promoter by Sp1 transcription factor binding (D'Addario et al. 2001). FLNa also protects cells from force-mediated apoptosis by preventing irreversible membrane depolarization (Kainulainen et al. 2002). In addition, the FLNa-mediated recruitment of FilGAP, into the lamellipodia enhances lamellae formation and the survival of the cells that are exposed to heavy tensile forces (Shifrin et al. 2009).

Increased stiffness of the collagen matrix regulates cell contraction and morphogenesis in some tissues. Cells are capable of sensing the stiffness of their environment and even modulating it. The level of FLNa-$\beta 1$ integrin interaction is increased in the cells that grow in the dense collagen environment that enhances the contraction of the collagen matrix and creates the equilibrium between the matrix stiffness and cell-generated matrix contractility (Gehler et al. 2009). Taken together, the results suggest that the FLNa-$\beta 1$ integrin complex acts as a mechanosensor that senses the mechanical forces generated by the ECM and induces cellular machinery to respond to those forces. Nevertheless, the detailed mechanisms of this mechanosensor function are not yet completely understood, and there are many conflicting results.

2.2.3.3 Filamin A in transcriptional regulation

Filamin A participates in transcriptional control by regulating the subcellular location of several transcription factors or their subunits. The effect of FLNa and transcription factor interactions changes from activating to inhibitory. FLNa interaction with the transcription factor subunit polyomavirus enhancer binding protein 2/core binding factor (PEBP2/CBFβ) retains it in the cytoplasm and thus inhibits its interaction with the nuclear Runx1 partner. PEBP2/CBFβ is

active only when the complex is formed. Therefore, the transcriptional activity of PEBP2/CBFβ is enhanced in FLNa-deficient cells (Yoshida et al. 2005). On the other hand, FLNa promotes the relocation of Smad proteins to the nucleus. Smads are involved in transforming growth factor β signaling pathway. They are phosphorylated in the cytoplasm by ligand-activated receptors and then accumulated into the nucleus. FLNa enhances both Smad phosphorylation and its translocation to the nucleus (Sasaki et al. 2001).

In several cell lines, both the full-length and the C terminal fragment of FLNa have been observed to locate in the nucleus, where they participate in transcriptional regulation. In androgen receptor-mediated signaling, the C terminal FLNa fragment containing domains 16-24 is cleaved by calpain and translocated to the nucleus. In the nucleus, the FLNa16-24 fragment represses the androgen receptor function by hindering its interaction with p60 coactivator transcriptional intermediary factor 22 (Ozanne et al. 2000, Loy et al. 2003). On the other hand, insulin-like growth factor-binding protein-5 induces the dephosphorylation-dependent cleavage of the FLNa16-24 fragment and its translocation to the nucleus. Thus, the FLNa16-24 fragment may serve as a shuttle of transcription factors and relocate them into the nucleus and finally promote the expression of insulin-like growth factor-binding protein-5 target genes, such as laminin γ1 (Abrass 2010). FLNa is also involved in the function of transcription factor forkhead box protein C1 in the nucleus, presumably through the relocation of the transcriptional regulatory protein, pre-B-cell leukemia transcription factor 1 (Berry et al. 2005). Consequently, the significant role of FLNa in transcription regulation has become evident when the nuclear expression of FLNa has been studied more. FLNa most likely serves as a scaffold also in the nucleus for transcription factors and their regulators, and thus affects their function either by enhancing or inhibiting their activity.

2.2.3.4 Filamin A in development

Several disease-causing mutations in the X chromosome-linked *FLNA* gene are known. They are divided into two groups. Nonsense and frameshift mutations of FLNa lead to periventricular nodular heterotopia (PVNH) triggered by the loss of FLNa function. Complete loss of FLNa function is lethal, and partial loss causes defects in the brain and cardiovasculature, including neuronal nodules in the lateral ventricle, epilepsy and malformations in blood vessels and the heart (Fox et al. 1998, Sheen et al. 2001).

The other group of *FLNA* mutation disorders is caused by a missense or gain-of-function mutation. In that case, the full-length FLNa is produced and its ability to bind to F-actin is retained. This otopalatodigital spectrum disorder (OPD) group includes OPD syndromes 1 and 2, frontometaphyseal dysplasia and Melnick-Needles syndrome. The symptoms range from mild skeletal dysplasia to lethal malformations in several tissues, including bones, blood vessels and the heart (Robertson 2007). The molecular mechanisms for OPD are mainly unknown. The OPD2 mutation E254K has been observed to reduce the

stability of FLNa ABD and to enhance the actin binding *in vitro.* Even then, the fibroblasts with FLNa E254K mutation move and adhere normally (Clark et al. 2009). The reasons for defects in bones of OPD 2 patients with E254K are still unclear.

The disorders caused by the *FLNA* gene mutation demonstrate the importance of FLNa during tissue and organ development. More information about the essential role of FLNa in various tissues has been gained by generating FLNa knockout mice. Complete depletion of the *FLNA* gene results in embryonic death. Intriguingly, actin assembly, cell extension formation and cell migration of various cell types in FLNa-null mice occur normally. Instead, the cell-cell junctions in vascular endothelial cells and epithelial cells are reduced, and the cell-cell junctions show abnormal morphology with complete loss of vascular endothelial cadherin. The impaired cell-cell contacts in vessels results in hemorrhage and defects in cardiac septation and other parts of the vascular system (Feng et al. 2006, Hart et al. 2006). The disruption of cell-cell junctions in neuroepithelial cells may also explain the accumulation of neurons at the ventricular surface in the brains of PVNH patients because the neuron migration is not disturbed in FLNa-null mice (Feng et al. 2006). In addition, skeletal malformations, such as cleft palate and sternum defects, are observed in FLNa-deficient mice (Hart et al. 2006). Even though the exact mechanisms of FLNa function during development are still unknown, FLNa is essential for proper development of multiple tissues and organs, including the brain, heart, blood vessels and bones.

3   AIMS OF THE STUDY

FLNa is a widely expressed actin-binding protein that links the actin cytoskeleton to the ECM through the transmembrane proteins. The appropriate function of FLNa is essential for cells as several malformations inducing patient mutations are known. Even if knowledge of the domain structures of filamins has recently increased, a considerable portion of the structural properties that have a significant effect on the function of filamins is still poorly comprehended. We examined the structure and function of FLNa domains and domain arrangement as well as FLNa interactions with its binding partners. The detailed aims of this research were as follows:

I. To find out the crystal structure of FLNa ABD and to reveal the exact location of patient point mutations in ABD.

II. To explore the atomic details of the interactions of the C terminal FLNa domains and their binding partners, such as migfilin, and to find out if a common interaction pattern exists.

III. To study the overall structure of C terminal rod 2 of FLNa. First, to examine if more domain pairs, besides the FLNa20-21 pair, exist and to determine the atomic structures of these pairs. Then, to reveal the overall structure and domain arrangement of the FLNa16-21 fragment.

IV. To clarify the effects of ligand binding on the conformation of FLNa16-21.
The methods used in this thesis are listed in Table 2 below. More detailed descriptions of the methods are given in the publications specified with Roman numerals.

4   SUMMARY OF THE METHODS

Table 2 summarizes the methods used in this thesis. A more detailed description can be found in the original publications.

TABLE 2   Methods

Method	Publication
DNA cloning	II, III, IV
QuikChange mutagenesis	IV
DNA sequencing	I, II, III, IV
Protein expression	I, II, III, IV
Protein purification	I, II, III, IV
SDS-PAGE[1]	I, II, III, IV
Crystallization	I, II
X-ray diffraction data collection and processing	I, II
Structure determination and refinement	I, II
Structure comparisons	I, II
Interaction surface analysis	I, II
SAXS[2] data collection and processing	III, IV
SAXS[2] *ab initio* modeling	III, IV
SAXS[2] rigid-body modeling	IV
Sequence alignment	III
Pull-down binding assays	III, IV
Size-exclusion chromatography	I

[1]sodium dodecyl sulfate polyacrylamide gel electrophoresis
[2]small-angle X-ray scattering

5 RESULTS AND DISCUSSION

5.1 The structure of filamin A actin-binding domain

When this study was started, there were no high-resolution structures of any FLN ABDs available. To reveal the atomic details of FLNa ABD and to figure out what the consequences of the known patient point mutations in this domain are at the atomic level, we expressed, purified and crystallized the ABD of FLNa. The crystal structure was determined with molecular replacement to 3.2 Å resolution using the structure of α-actinin 1 ABD (PDB code 2EYI, Borrego-Diaz et al. 2006) as the search model. The FLNa ABD adopts a compact, closed conformation where two CH domains lie adjacent to each other (Fig. 7B). The interaction surface of these two CH domains is ~800 Å^2. Each CH domain contains four predominant (A, C, E and G) and two minor (B and F) helices. Poor electron density in the most N terminal part (residues 1-40) and in the flexible linker between the CH domains (residues 155-165) prevented the model building of these regions. The overall folding pattern of FLNa ABD is conserved with previous ABDs, especially the recently published structure of FLNb ABD (PDB code 2WA5, Sawyer et al. 2009) is highly similar with a root mean square deviation (rmsd) of 0.425 Å (211 C$^\alpha$ atoms).

Although the detailed structure of the F-actin-ABD complex is not known, mutagenesis studies have suggested three distinct ABSs in ABDs (Bresnick et al. 1991, Kuhlman et al. 1992, Lebart et al. 1994). Thus, it is useful to consider the location and characteristics of these segments in FLNa ABD. Based on the sequence alignment, two ABSs in FLNa ABD are located in the CH1 domain. ABS1 is composed of residues 46-55, and ABS2 residues 130-149, respectively. ABS3 (173-192) is situated in the first helix of the CH2 domain (Fig. 7B). In FLNa, ABS1 has been mostly hidden between the CH domains, suggesting that some conformational rearrangement has to occur in FLNa ABD to allow F-actin binding.

There are two FLNa ABD molecules in the asymmetric unit of the crystal (Fig. 7A). The interaction surface of the ABD molecules is remarkably large (~1250 Å^2), composed of 11 hydrogen bonds and 15 salt bridges, proposing rather tight interaction and dimer formation in solution conditions. In size

exclusion chromatography, the ABD came out as a single peak with a retention volume of 13.37 ml, which, based on the molecular weight standard, indicates the molecular weight of ~54 kDa. Since the molecular weight of FLNa ABD monomer is only 31 kDa, this finding supports the dimeric conformation of FLNa ABD in solution.
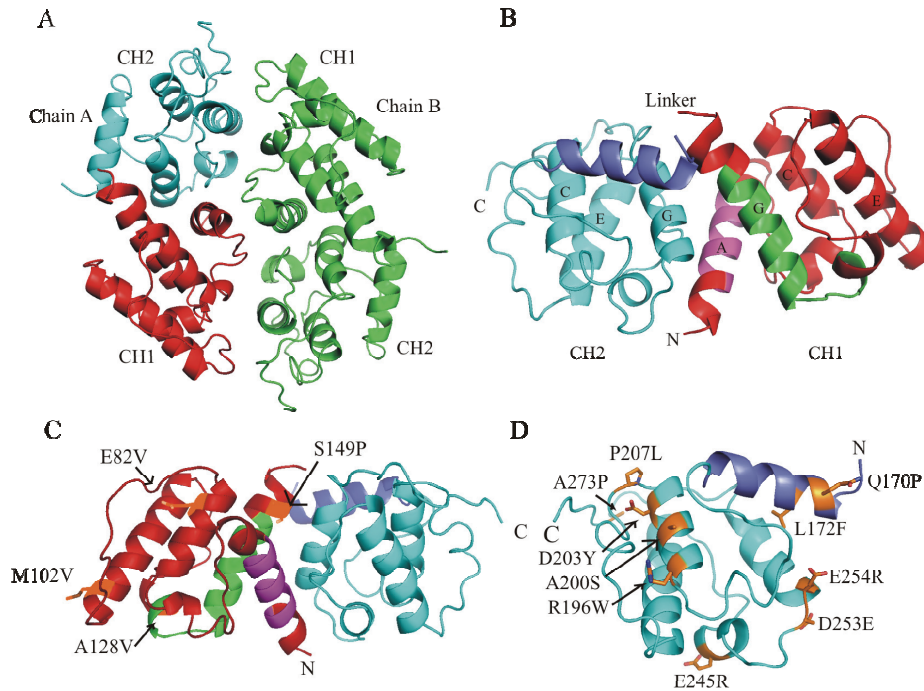

FIGURE 7   A. The asymmetric unit of the FLNa ABD crystal contains two ABD chains. The CH1 of chain A is presented in red and CH2 in cyan while chain B is displayed in green. B. The structure of FLNa ABD in which four predominate helices in both CH domains are marked and ABS1 is shown in purple, ABS2 in green and ABS3 in blue. C. PVNH-causing point mutations are highlighted and displayed as sticks and in orange. D. Point mutations causing the OPD syndrome disorders are marked in CH2.

5.1.1 Location of patient mutations in the actin-binding domain

Mutations in the *FLNA* gene cause multiple disorders that disrupt the normal development of the bones, blood vessels, heart or brain. Some of these mutations cause large changes, including deletion, insertion, nonsense or frameshift mutations, but several congenital-disease-causing point mutations in *FLNA* are also known. We examined the exact location of PVNH and OPD spectrum disorders (p. 22) causing point mutations in FLNa ABD and considered the effect of the amino acid mutations on ABD folding and actin binding.

The loss-of-function mutations in the *FLNA* gene cause PVNH (see p. 21) (Fox et al. 1998, Sheen et al. 2001). Four PVNH-causing point mutations in FLNa ABD have been found thus far; E82V, M102V, A128V and S149P. They are all located in the CH1 domain, but none of them is directly in the ABSs (Fig. 7C). The E82V and M102V mutations affect the surface-exposed amino acids distant from CH2 and point away from ABSs. The dramatic effects of these mutations may be based on the alteration in the chemical properties of the ABD surface. On the contrary, A128V and S149P mutations are situated in or near the α helices that contribute to actin binding and can be predicted to disrupt ABS2.

The OPD spectrum disorders (see p. 21) are all caused by gain-of-function mutations in *FLNA* while the full-length FLNa protein is found in the cells of these patients (Robertson 2007). All OPD1 and 2 and two frontometaphyseal dysplasia-causing mutations are concentrated in the CH2 domain. The mutated residues represent both surface-exposed and embedded residues and are rather widely dispersed around the domain (Fig. 7D). There are two mutations in the area of ABS3, Q170P and L172F, that both presumably disrupt the conformation of the α helix and directly affect the actin-binding properties of ABS3. Patient mutation residue D253 lies between the CH domains on their interaction surface and may hinder the interaction of CH1 and CH2 and affect the overall conformation of ABD. Other patient mutations (R196W, A200S, D203Y, P207L, E245R and A273P) probably have local effects on the folding or surface properties of ABD. The recently published crystal structure of FLNa ABD with E254K patient mutation (PDB code 2HOC, Clark et al. 2009) shows that the mutation disrupts the highly conserved salt bridge between the residues K166 and E254, causing the exposure of some hydrophobic residues (F188 and M258) in domain core. Although, the overall fold of ABD remains the same, the actin binding affinity of E254K mutant is significantly increased (Clark et al. 2009). To conclude, only two patient mutations lie directly in ABS, although many of them presumably affect the actin-binding affinity of FLNa. Otherwise, indirect effects, including changes in the chemical properties of ABD surface or conformational changes in some part of ABD, cause the altered actin-binding properties of the mutants.

5.2   The interaction of filamin A and migfilin

Migfilin is a newly found adaptor protein that binds to all human FLNs. It participates in cell adhesion and migration together with FLNa (Takafuta et al. 2003, Tu et al. 2003). We wanted to reveal more about migfilin-FLNa interaction and its effects on important cell functions. Pull-down assays showed that FLNs bind to the most N terminal portion of migfilin that lacks known structural domains or motifs (II, Fig. 1). Based on the sequence alignment, mutagenesis studies and nuclear magnetic resonance (NMR) spectroscopy interaction assays the FLN binding site in migfilin was further narrowed down to residues 5-19 (II,

Fig. 3). In FLNa, there are several migfilin binding sites while both the ABD + rod 1 fragment and the rod 2 fragment bound to migfilin in pull-down assays. The primary binding site was, however, found in FLNa21 (II, Fig. 2).

Migfilin is localized both in actin stress fibers and in cell-ECM adhesions in cells (Tu et al. 2003). The deletion of the FLN binding region, residues 1-85, causes migfilin accumulation in adhesion sites, supporting the assumption that FLNs mediate the localization of migfilin to actin filaments. On the contrary, a migfilin fragment containing only the most N terminal part (1-85) predominantly localizes in stress fibers but not in adhesions (II, Fig. 7). The migfilin localization in adhesion sites is presumably mediated by kindlin-2 that binds to integrin β tails and to migfilin (Tu et al. 2003).

5.2.1 The structure of the filamin A domain 21-migfilin complex

To find out the atomic details of the FLNa21-migfilin interaction we co-crystallized a migfilin peptide containing residues 5-19 with FLNa21. The crystals belonged to the $P2_12_12_1$ space group and diffracted to 1.9 Å resolution. The complex structure was solved using molecular replacement with the structure of FLNa21 from the FLNa21-integrin β7 complex structure (PDB code 2BRQ, chain A, Kiema et al. 2006). There are two FLNa21 molecules and one migfilin peptide in the asymmetric unit of the crystal (Fig. 8A). FLNa21 molecules were highly similar to each other (rmsd 0.245 Å for 353 atoms) and to FLNa21 of the integrin β7 complex (rmsd 0.388 Å for 345 atoms). In the asymmetric unit, a single migfilin peptide is situated between two FLNa21 molecules, interacting with them slightly differently (Fig. 8A). However, the interaction surface of both FLNa21 molecules is the CD face and migfilin forms an extra β strand next to the C strands of both FLNa21 molecules (Fig. 8C). The side chains of migfilin residues S11, V13 and I15 interact with FLNa21 chain A (Fig. 8B), while the side chains of residues S12, F14 and T16 form the interaction to chain B, respectively. To test which interaction mode is biologically relevant, the binding of migfilin peptides with mutations in appropriate residues (S11, S12, F14 and I15) was tested using NMR spectroscopy and pull-down binding assays. Point mutations in residues S11 and I15 of migfilin hindered the FLNa21 binding in pull-down assays. Migfilin peptides with these mutations also exhibited fast or intermediate exchange behavior, typical for weak interactions, in NMR binding assays while S12 and F14 mutations had no effect (II, Fig. 5). These findings show that the interaction mode between FLNa21 chain A in the crystal and the migfilin peptide is the dominant interaction in solution. This interaction mode was also later confirmed with NMR (Ithychanda et al. 2009a), and the interaction highly resembles the FLNa21 interaction with integrin β tails (Kiema et al. 2006, Takala et al. 2008) and the cystic fibrosis transmembrane conductance regulator (Smith et al. 2010). In addition, other odd-numbered C terminal FLNa domains utilize a similar kind of interaction pattern when interacting with their binding partners; for example, FLNa17 binds to glycoprotein Ibα (GPIbα) (Nakamura et al. 2006) and FLNa23 to FilGAP with a

comparable mechanism (Nakamura et al. 2006, Nakamura et al. 2009). The common binding mechanism of FLNa C terminal Ig-like domains could, thus, be confirmed.

The FLN binding sites of integrin β tails and migfilin are convergent (Kiema et al. 2006, Takala et al. 2008). The observed dissociation constants vary depending on the assay, but migfilin constantly has higher affinity for FLNa21 (0.5-2.3 μM) (Ithychanda et al. 2009b) than integrin β7 (0.7-40 μM) (Kiema et al. 2006, Lad et al. 2007, Ithychanda et al. 2009a, Ithychanda et al. 2009b) or integrin β2 (525 μM) (Takala et al. 2008). We tested if migfilin can compete with integrin β7 for FLNa21 binding. As predicted, the dose-dependent inhibition of integrin β7 binding to FLNa21 was observed when migfilin was added (II, Fig. 6). Competition between integrin and migfilin may thus provide a regulation mechanism of FLNa interactions that may control integrin-mediated cell adhesion and signaling.
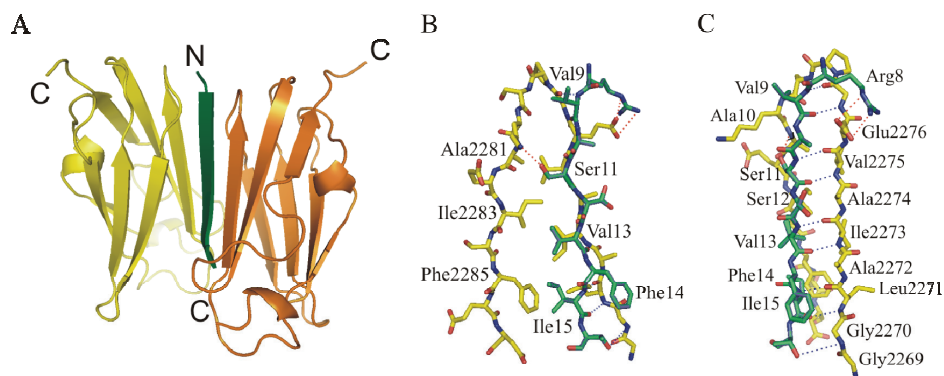
FIGURE 8   A. In the asymmetric unit of the crystal, there are two FLNa21 chains, A (yellow) and B (orange), and the migfilin peptide (green) is located between the FLNa21 molecules. B. In a biologically relevant interaction, S11 of migfilin forms a hydrogen bond to FLNa21 chain A while the other migfilin side chain interactions are mainly hydrophobic. C. The migfilin peptide forms an extra β strand next to the C strand of FLNa chain A.

5.3 The domain arrangements in the filamin A rod 2 region

The C terminal rod 2 region of FLNa includes domains 16-24. In electron microscopy studies, this fragment has been shown to be more compact than expected for nine independently folded Ig-like domains (Nakamura et al. 2007).

5.3.1 The low-resolution structures of two domain fragments

TABLE 3 The R_g and D_{max} values of FLNa fragments

Sample	$R_g{}^1$ (nm)	$D_{max}{}^2$ (nm)
FLNa12-13	2.39 ± 0.01	9
FLNa16-17	1.93 ± 0.03	6
FLNa18-19	2.11 ± 0.04	7
FLNa20-21	1.91 ± 0.03	6
FLNa22-23	2.77 ± 0.05	9
FLNa1621	3.42 ± 0.01	12
FLNa1521	4.07 ± 0.01	15
FLNa16-21+integrin β2	3.47 ± 0.01	12
FLNa16-21+migfilin	4.08 ± 0.02	14
FLNa16-21+migfilin x 2	3.68 ± 0.01	13
FLNa16-21+migfilin I15E	3.40 ± 0.01	11
FLNa16-21+DR D3	3.90 ± 0.01	15
FLNa16-21+DR D3+migfilin	4.21 ± 0.01	15
FLNa16-21 I2144E	3.60 ± 0.01	11
FLNa16-21 I2144E+integrin β2	3.67 ± 0.01	13
FLNa16-21 I2144E+migfilin	3.95 ± 0.02	13
FLNa16-21 L1956E	3.60 ± 0.02	12
FLNa16-21 L1956E+DR D3	4.03 ± 0.01	13
FLNa16-21 L1956E I2144E	3.65 ± 0.01	12
FLNa16-21 L1956E I2144E+DR D3+migfilin	5.11 ± 0.02	17

[1]R_g, radius of gyration; R_g errors were computed by Primus

[2]D_{max}, maximum linear dimension, errors ~10 %

The crystal structure of FLNa19-21 reveals that domains 20 and 21 fold co-operatively and thus form a compact domain pair in which FLNa20 lies on top of FLNa21. In this unforeseen domain arrangement, the FLNa20 A strand interacts with the CD face of FLNa21 and masks the known binding site (Lad et al. 2007). The sequence alignment of FLNa domains reveals that the even-numbered domains 16, 18, 20 and 22 of FLNa rod 2 differ from all other FLN domains especially in the expected A strand (Gorlin et al. 1990). Based on these facts, we wanted to find out if other domain pairs similar to FLNa20-21 also exist elsewhere in rod 2. Therefore, we cloned, expressed and purified five two domain FLNa fragments containing domains 12-13, 16-17, 18-19, 20-21 and 22-23. The fragment 12-13 was used as a control since the domain pair formation was not expected in FLNa rod 1. The small-angle X-ray scattering (SAXS) data for FLNa fragments was measured. All fragments behaved well in SAXS, and no aggregation was observed. The experimental scattering curves and distance distribution functions of FLNa16-17, 18-19 and 20-21 resembled each other and suggested the rather globular shape of the particles (III, Fig. 2). Both the radius of gyration (R_g) and the maximum linear dimension (D_{max}) of FLNa16-17 and 18-19 are in the same range, 1.93-2.11 nm and 6-7 nm, as the values of the known domain pair 20-21, 1.91 nm and 6 nm (Table 3). In contrast, the R_g and

D_{max} values of FLNa12-13 and 22-23 were remarkably higher (Table 3), and the scattering curves (III, Fig. 2) and distance distribution functions also indicated a more elongated shape (III, Fig. 2, inserts). The D_{max} values of FLNa12-13 and 22-23 are consistent with the dimension of two independently folded Ig-like domains.

The *ab initio* envelopes of the two domain FLNa fragments are shown in Fig. 9. They all fitted well to the experimental SAXS data, giving the discrepancy factors of 1.69-1.87. The shape of the FLNa18-19 and 20-21 envelopes is rather similar, showing an extension at the end of envelope, while the FLNa16-17 envelope is more globular and compact. The FLNa12-13 and 22-23 envelopes differ significantly from the other pairs. These envelopes are more elongated and thinner, representing the head-to-tail packing of two domains. These results suggest that FLNa16-17 and 18-19 also form rather globular and compact domain pairs, but in FLNa22-23, as well as in the control fragment 12-13, Ig-like domains do not fold co-operatively but exist as distinct domains.
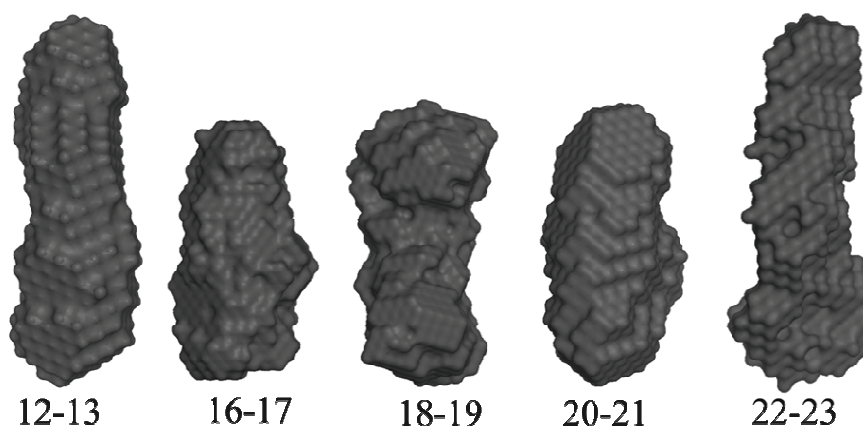

FIGURE 9   The *ab initio* envelopes of FLNa two domain fragments 12-13, 16-17, 18-19, 20-21 and 22-23 displayed in the same scale.

5.3.2 The high-resolution structure of filamin A domains 16-17

To reveal the atomic details of domain pairs FLNa16-17 and 18-19, observed in SAXS, NMR spectroscopy was utilized. The NMR studies of FLNA16-17 showed that these domains tightly interact with each other. Surprisingly, the overall folding pattern of this domain pair is completely different from the previously seen pair, FLNa20-21. Domains 16 and 17 lie parallel next to each other, forming a relatively large (~720 Å^2) interaction surface that could be confirmed by 99 interdomain distance restraints in NMR (Fig. 10A). The expected A strand of FLNa16 is unstructured and is not folded with the rest of domain. This exposes the hydrophobic BG face of FLNa16. This BG face interacts with the FLNa17 A and G strands that contain numerous aromatic and

hydrophobic residues. Accordingly, the FLNa16-17 interaction is mainly based on the hydrophobic effects instead of hydrogen bonding. The structure suggests that the known GPIbα binding site, the CD face, in FLNa17 is not masked by FLNa16. To verify this, we employed the pull-down binding assays with the GP1bα peptide and the FLNa16-17 and FLNa17 fragments. The assays showed that the binding affinities to GP1bα of the domain pair and the single domain are equal (10-20 μM). The binding affinity of FLNa17 is consistent with those reported before (Nakamura et al. 2006). This confirms that FLNa16 does not interact with the CD face of FLNa17 but binds to the AG face of the same domain. The folding pattern of FLNa16-17 is thus completely distinct from the previous Ig-like domain containing multidomain structures.
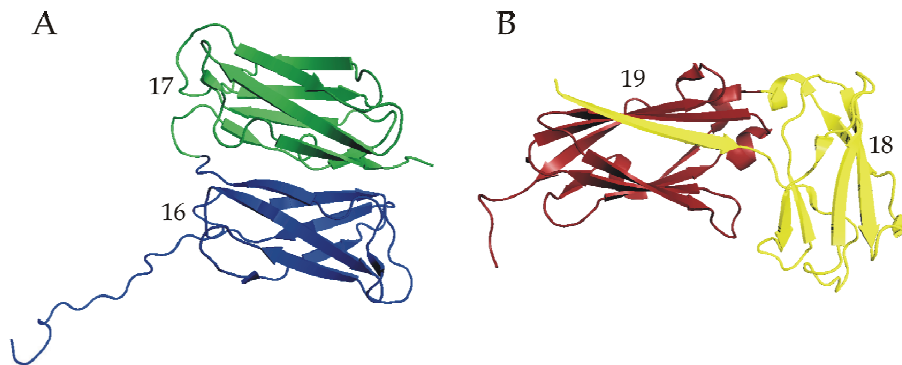

FIGURE 10 The atomic structures of FLNa16-17 (A) and 18-19 (B) domain pairs.

5.3.3 The high-resolution structure of filamin A domains 18-19

The SAXS measurements showed that the shape and distances of FLNa18-19 significantly resemble those of the FLNa20-21 domain pair (Fig. 10). The atomic structure of FLNa18-19 was solved with solution state NMR spectroscopy to find out if the domain packing is analogous to FLNa20-21. In the determination of mutual orientation of domains FLNa18 and 19, 76 interdomain distance restraints were employed. The overall domain arrangement of FLNa18-19 is highly similar to that of FLNa20-21. FLNa19 is folded like a typical Ig-like domain composing of seven β strands while FLNa18 is positioned on the top of FLNa19 interacting with the BC loop of FLNa19 (Fig. 10B). The main interacting residue is the conserved Y2077 in the BC loop of FLNa19 (III, Fig. 4D). It points outwards from the loop and interacts with the several hydrophobic residues of the FLNa18 AB loop (A1969, I1971), D strand (F2011, P2013) and G strand (V2037, I2039). In the FLNa20-21 pair, the main interaction surface of domain 20 is the G strand. Thus, the relative orientation of the two domains differs in the tandem domain pairs of FLNa18-19 and 20-21 (III, Fig. 7).

The A strand of FLNa18 does not fold together with the rest of the same domain but forms an additional β strand adjacent to the C strand of FLNa19. This resembles the arrangement in FLNa20-21 (Lad et al. 2007). In addition to

main chain hydrogen bonding, the S1961 of the FLNa18 A strand forms the hydrogen bond to the D strand of FLNa19. In addition, numerous hydrophobic side chain contacts maintain the interaction between the FLNa18 A strand and the FLNa19 CD face. The CD face of FLNa19 is the second binding site of integrin β tails in FLNa. In the NMR binding studies, integrin β7 peptide did not bind to the FLNa18-19 fragment while binding to FLNa19 was clearly observed (III, Supplemental Fig. S4). This finding confirms the masking of the CD face of FLNa19 by the A strand of FLNa18 (Lad et al. 2007).

5.3.4 The overall structure of the filamin A rod 2 region

According to the data presented above, the six domain fragment, FLNa16-21, contains three tandem domain pairs. Based on the sequence alignments, this six-domain fragment, which follows the first hinge region, seems to be evolutionally conserved throughout the animal kingdom. This fragment can be found in all vertebrate FLNs that have 24 Ig-like domains; in addition, *Drosophila melanogaster* (Cherio) and *Caenorhabditis elegans* (Y66H1B) FLNs include a similar kind of fragment close to their C terminus. Although the total number of Ig-like domains in the fruit fly and earthworm FLNs is smaller than in vertebrates, the exact distance of these three tandem domain pairs from the C terminus remains fixed. The evolutionary conservation of the three tandem domain pairs in FLNs proposes the functional significance of these structures.

Although the atomic structures of two or three domain fragments had been determined, the structure and domain arrangement of entire six domain fragment, FLNa16-21, were still unknown. To reveal the domain assembly of this region, we measured the SAXS data for FLNa16-21. FLNa16-21 showed neither oligomerization nor aggregation in SAXS and gave the scattering profile and distance distribution function typical for a complex and branched particle instead of indicating an elongated shape. In addition, the R_g (3.42 nm) and D_{max} (12 nm) of FLNa16-21 suggested a rather compact domain arrangement when compared to those of single domain pairs (R_g 1.91-2.11 nm, D_{max} 6-7 nm) (Table 3).

The shape of FLNa16-21 was reconstructed based on the scattering data using the program GASBOR (Svergun et al. 2001). The single models that fitted to the experimental data with discrepancy factors 1.1-1.7 were then averaged and filtered to achieve the most populated volume. The *ab initio* envelope of FLNa16-21 exhibits a planar, three-branched shape with equally long arms (Fig. 11A).

The atomic structures were fitted to the SAXS data using rigid-body modeling. For this, experimental scattering data from FLNa16-21 was used with or without data from the fragment containing domains 16-19 and 18-21. The fits to experimental data in both cases were excellent, and no significant difference between the models was observed. The modeling was tested using either single domains or domain pairs as rigid bodies. The model generated using three domain pairs, FLNa16-17, 18-19 and 20-21, was highly reproducible and gave a

remarkably good fit to the experimental data with the discrepancy factor 0.91. If the single domains were used, the fit was not sufficient while the discrepancy factor increased to over three. The rigid-body model shows that FLNa16-21 has adopted a three-branched domain arrangement in which each domain pair forms one of the three arms (Fig. 11A, B, C). The overall shape of the rigid-body model is congruent with the *ab initio* envelope (Fig. 11A). NMR studies showed notable differences in the spectra of the domain pairs depending if they were measured as isolated pairs or as a part of the FLNa16-21 fragment. This indicates that domain pairs remain unchanged also in longer FLNa fragments, as in FLNa16-21, and do not have any considerable interactions with adjacent domain pairs.

Our compact model of FLNa16-21 is consistent with the previous electron microscopy studies that illustrate that C terminal domains, FLNa16-24, are more compactly packed than rod 1 domains (Nakamura et al. 2007). If the distances of the FLNa16-21 model and the FLNa22-23 *ab initio* envelope are counted up and the location of the C terminus of FLNa21, in the middle part of FLNa16-21, is taken into account, the length of FLNa16-23 would be ~15 nm. However, the length of FLNa16-23 in electron micrographs was 19.2 ± 6 nm (Nakamura et al. 2007). The platinum shadowing may affect the EM measurements while the thickness of the appropriate platinum layer in most cases is ~1.0-3.0 nm (Wepf et al. 1991, Stokroos et al. 1998).
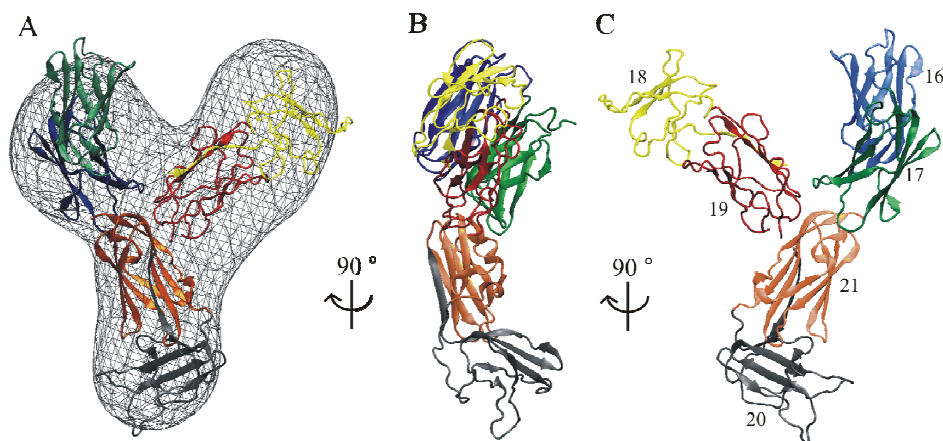

FIGURE 11 The rigid-body model of FLNa16-21 shown from three different angles (A, B, C). A The rigid-body model fitted into the *ab initio* envelope (grey) of FLNa16-21. FLNa16-21 forms a compact, planar and three-branched fold that fits well into the *ab initio* envelope. Domains are shown as cartoon and in different colors.

5.4   Conformational changes in the filamin A rod 2 region

The interactions of FLNa are concentrated in rod 2 as the majority of the FLNa binding partners interact with the C terminal domains and particularly with the CD faces of odd-numbered domains. However, the known binding sites in FLNa19 and 21 are masked by the first strand of previous domains, both in domain pair structures and in the FLNa16-21 model (Lad et al. 2007, III, IV). Nevertheless, integrins (Loo et al. 1998), migfilin (Tu et al. 2003) and DR D3 (Li et al. 2002) can bind to full-length FLNa. This suggests that some domain rearrangement takes place in FLNa16-21 when it binds to ligands. To observe the conformational changes on FLNa16-21, we measured scattering data for FLNA16-21 also in the presence of DR D3, migfilin and integrin β2 cytoplasmic tail peptides. Both DR D3 and the migfilin peptide induced an increase in the R_g of FLNa16-21 (from 3.42 nm to 3.90 or 4.09 nm) as well as in D_{max} that increased by 2-3 nm (Table 3), indicating some changes in the overall conformation of FLNa16-21. In addition, the scattering profiles and distance distribution functions of FLNa16-21 are distinct from those measured in the absence of peptides (IV, Supplemental Fig. S3). A mutant migfilin (I15E) that does not interact with FLNa (II) had no effect either on R_g or D_{max} (Table 3), suggesting that the migfilin binding mechanism to FLNa16-21 is the same as to the single FLNa21 domain.

For migfilin to bind, the A strand of FLNa20 has to detach from the CD face of FLNa21. To study the role of FLNa18 and FLNa20 in the interactions, we introduced A strand interaction loosening mutations to FLNa18 (L1956E) or FLNa20 (I2144E). The pull-down binding assays confirmed the effect of the FLNa20 A strand mutation on the FLNa16-21-migfilin interaction; two-fold enhancement of migfilin binding was observed upon the I2411E mutation in FLNa16-21 (IV, Fig. 3A, C). This finding is consistent with the increased binding of the FLNa19-21 I2144E mutant to the integrin β7 tail compared to the wild type (Lad et al. 2007).

In SAXS, the A strand mutations (L1956E and I2144E) alone did not induce any change on FLNa16-21, but in the presence of DR D3 or the migfilin peptide, as well as the integrin β2 peptide, increases in R_g and D_{max} were observed. The integrin peptide induced changes only if the FLNa20 A strand interaction with the CD face of FLNa21 had been hindered (Table 3). A sufficient model with a discrepancy factor of 1.91 for migfilin-bound FLNa16-21 was generated using the data from domains FLNa16-21 with 20 A strand mutation (I2144E) and migfilin peptide by combining *ab initio* and rigid-body modeling. In the model, the FLNa20 A strand is detached from FLNa21 and forms a flexible linker between the FLNa19 and the rest of the FLNa20. The whole FLNa16-21 is thus less compact (Fig. 12). The most evident changes in the conformation of FLNa16-21 were, however, seen when both DR D3 and the migfilin peptide and both A strand mutations were introduced. The scattering profile and distance distribution function of this fragment were typical for an elongated and

unbranched particle (IV, Fig. 4) and R_g and D_{max} increased by 1.69 and 5 nm (Table 3), respectively. This reveals that the binding of DR D3 or migfilin peptide induces a rather large conformational change in FLNa16-21. The change is caused by a detachment of the single A strand or both A strands from the CD faces of odd-numbered domains (IV, Fig. 5). Whether the binding sites in FLNa19 and 21 are independently regulated as the FLNa16-21 model indicates, however, is still uncertain. The finding that the integrin β2 peptide was not able to induce conformation change in FLNa16-21 without the A strand loosening mutation is consistent with its lower affinity compared to migfilin.
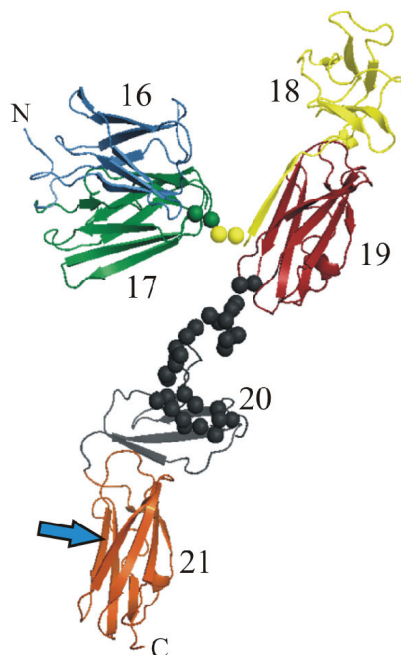

FIGURE 12   The model for migfilin-bound FLNa16-21 in which the FLNa20 A strand has been detached from the migfilin binding site, the CD face of FLNa21 (pointed by the blue arrow). The flexible linkers between the domain pairs and the FLNa20 A strand are represented as dummy residues.

Taken together, these results show that the structure of the FLNa16-21 fragment is rather compact but flexible and the domain arrangement can change, for example, through the ligand binding. The other possibility is that in cells mechanical forces elicit conformational changes in the rod 2 region of FLNa, thus facilitating ligand binding (Pentikäinen & Ylänne 2009). This provides a mechanism for the role of FLNa as a mechanosensor in cells.

    Thus far most findings of the conformational flexibility of FLNs are based on the molecular level *in vitro* assays. Even though the cellular studies of this kind of dynamic conformational changes in proteins are not straightforward, it will be important to be able to investigate this phenomenon also in cells in the future. In the *in vitro* assays, the predominant conformation of FLNa rod 2 is the

tightly packed form with three domain pairs and masked binding sites. Some results indicate that this domain arrangement also dominates in cells but further studies are needed to find out more about the regulation mechanisms of the conformational changes in FLNs and their effects on the cell functions.

6 CONCLUDING REMARKS

The main conclusions of this thesis are as follows:

I. FLNa ABD contains two highly conserved CH domains and adopts a closed conformation in which ABSs are partially embedded. The patient point mutations in the FLNa ABD presumably have direct effects on actin binding and indirect effects that affect the domain function through the changes in the domain conformation or chemical properties of the domain surface.

II. Migfilin binds to the CD face of FLNa21. It forms an additional β strand adjacent to the C strand of FLNa21 while migfilin side chains interact with FLNa D strand side chains. The interaction site and mode are congruent with those of integrins and highly resemble several other FLN Ig-like domain interactions, confirming the existence of their common interaction pattern.

III. There are three tandem domain pairs in rod 2 of FLNa while domains 16-17, 18-19 and 20-21 fold co-operatively, but domains 22 and 23 exist as typical distinct Ig-like domains. In FLNa18-19, the first strand of domain 18 masks the CD face binding site of FLNa19 as in the FLNa20-21 domain pair. The FLNa16-17 domain pair folds completely differently; no binding masking occurs. The FLNa16-21 fragment forms a planar, rather compact and three-branched fold in which each arm is composed of one domain pair, suggesting pair formation in longer FLNa fragments.

IV. Large conformational changes in FLNa16-21 are induced by FLNa ligands such as DR D3, migfilin and integrin. They occur when FLNa18 and FLNa20 A strand interaction with the CD faces of FLNa19 and FLNa21 are weakened. This is consistent with the displacement of the A strands by the ligands that can change the overall conformation of the six-domain segment from three-branched to a long, elongated rod. Similar conformational changes are possible during mechanical stretching, thus providing a mechanism for the mechanosensory function of FLNa.

Acknowledgements

Now, the work is done and I want to express my gratitude to all the people who somehow helped me with this long project. First, I thank my supportive supervisor, Professor Jari Ylänne, who has guided me into the scientific world. I am especially grateful to Jari for giving me an opportunity to do things independently, my way, and for being strict enough to keep me going.

Docents Pirta Hotulainen and Tiina Salminen reviewed this thesis. I thank them for their constructive feedback. I am also grateful to my thesis committee members, Pirta and Professor Pirkko Heikinheimo, for their advice.

I had the privilege to work on a good group with great groupmates. I give my thanks to Ulla for her help with the long filamin fragments. She taught me a great deal about research and I think we were a good team. I also thank my long-term roommate, Heikki, who has shared most of the good and bad moments with me. He has helped me a lot and always made sure that I kept my feet on the ground. I also acknowledge the JY group's other members, Fabiana and Ritika.

I worked in collaboration with many skillful scientists. I express my gratitude to Peter Konarev and Dmitri Svergun (EMBL Hamburg); to Professor Iain Campbell's group (University of Oxford); and to Outi Koskela, Docent Perttu Permi and Professor Ilkka Kilpeläinen (University of Helsinki). I am extremely grateful to Assistant Professor David Calderwood (University of Yale), who made my research visit to Yale possible. I also want to thank Mohamed Bouaouina for his help in the lab and Ziba Razinia for the sightseeing tours and other activities during my visit.

Next, I want to thank the person who has helped me most in the lab. I am extremely grateful to Arja "Allu" Mansikkaviita for all the advice she gave me. I also thank her for helping me express and purify my proteins. I thank Docent Olli Pentikäinen for his help with Linux programs. I also want to thank Emilia Horttana and Kati Viitaniemi for the DNA cloning, mutagenesis and protein purification they made for me. I am especially grateful to Kati for making my long lab days more fun and exciting. I also thank the rest of "the gang of the C2 wing," Elisa, Moona, Mikko, Lassi, Heli, etc., and the ISB's members for all the entertaining moments. It is impossible to list them all here.

I express my deep gratitude to my parents for all the support and encouragement they have given me. I also thank my brother Miika, my grandparents and my friends. Finally, I give enormous thanks to Jarkko for his help, support, patience and love, particularly during the writing process. I also want to thank Jarkko for all those marathon discussions, not only about science, but also about life.

YHTEENVETO (RÉSUMÉ IN FINNISH)

Filamiinidomeenien rakenteet, vuorovaikutukset ja pakkautuminen

Filamiinit ovat suurikokoisia proteiineja, jotka yhdistävät solun aktiinisäikeitä kolmiulotteiseksi verkostoiksi ja kimpuiksi sekä toimivat kiinnittymisalustana muille proteiineille. Filamiinit osallistuvat solun tarttumiseen, liikkumiseen, viestinvälitykseen ja transkription säätelyyn. Filamiinigeenien mutaatiot aiheuttavat useita sairauksia, joissa esiintyy aivojen, luuston sekä sydän- ja verisuonielimistön kehityshäiriöitä. Ihmisen filamiinit koostuvat polypeptidiketjun aminopäässä olevasta aktiiniin sitoutuvasta domeenista ja 24 immunoglobuliinin kaltaisesta domeenista. Immunoglobuliinin kaltaiset domeenit muodostavat pitkän sauvamaisen rakenteen, joka jakautuu kahteen osaan. Ensimmäisen sauvamaisen osan muodostavat domeenit 1-15 ja toisen domeenit 16-24. Nämä osat erottaa toisistaan joustava sarana-alue. Filamiinin toiminnallinen yksikkö muodostuu kahdesta samanlaisesta polypeptidiketjusta, jotka sitoutuvat toisiinsa karboksyylipäässä olevan immunoglobuliinin kaltaisen domeenin välityksellä.

Tässä väitöskirjassa ratkaistiin filamiini A:n aktiiniin sitoutuvan domeenin kiderakenne, joka paljasti konservoituneen laskoksen sisältäen kaksi kalponiinihomologiadomeenia. Rakenteen perusteella tarkasteltiin aktiiniin sitoutuvassa domeenissa sijaitsevien potilasmutaatioiden sijaintia. Sijainnin perusteella pohdittiin niiden vaikutuksia domeenin konformaatioon ja aktiinin sitomiskykyyn. Lisäksi ratkaistiin filamiini A:n domeenin 21 kiderakenne yhdessä migfiliinin kanssa. Rakenteessa havaittiin, että migfiliini sitoutuu filamiini A:han samankaltaisesti kuin useat muut filamiiniin sitoutuvat proteiinit osoittaen, että filamiinien immunoglobuliinien kaltaisilla domeeneilla on yhteinen sitoutumismalli.

Useat filamiiniin vuorovaikutuskumppanit sitoutuvat karboksyylipäässä olevaan toiseen sauvamaiseen alueeseen. Tässä työssä osoitimme, että kyseisellä alueella on kolme tiiviisti pakkautunutta domeeniparia. Yksi tunnettiin aikaisempien tutkimusten pohjalta. Näistä pareista kaksi sisältää sitoutumiskohdan, joka on peittynyt domeenien väliin. Tutkimustemme mukaan tämä kuuden domeenin pala muodostaa tiiviisti pakkautuneen, kolmihaaraisen rakenteen, jonka konformaatio kuitenkin muuttuu merkittävästi sen sitoutuessa vuorovaikutuskumppaneihinsa. Konformaatiomuutoksen aiheuttama sitoutumispaikkojen paljastuminen saattaa toimia keinona säädellä filamiinin vuorovaikutuksia ja tukee filamiinin roolia soluun kohdistuvien mekaanisten voimien sensorina. Solussa erilaisten voimien aiheuttama filamiinin venyminen voi saada aikaan vastaavanlaisen sitoutumispaikkojen paljastumisen ja siten säädellä filamiinin sitoutumista muun muassa säätelyproteiineihin.

REFERENCES

Anilkumar, G., Rajasekaran, S. A., Wang, S., Hankinson, O., Bander, N. H. & Rajasekaran, A. K. 2003. Prostate-specific membrane antigen association with filamin A modulates its internalization and NAALADase activity. Cancer Res. 63: 2645-2648.

Armstrong, L. J., Heath, V. L., Sanderson, S., Kaur, S., Beesley, J. F., Herbert, J. M., Legg, J. A., Poulsom, R. & Bicknell, R. 2008. ECSM2, an endothelial specific filamin a binding protein that mediates chemotaxis. Arterioscler. Thromb. Vasc. Biol. 28: 1640-1646.

Awata, H., Huang, C., Handlogten, M. E. & Miller, R. T. 2001. Interaction of the calcium-sensing receptor and filamin, a potential scaffolding protein. J. Biol. Chem. 276: 34871-34879.

Baldassarre, M., Razinia, Z., Burande, C. F., Lamsoul, I., Lutz, P. G. & Calderwood, D. A. 2009. Filamins regulate cell spreading and initiation of cell migration. PLoS One 4: e7830.

Banuelos, S., Saraste, M. & Djinovic Carugo, K. 1998. Structural comparisons of calponin homology domains: implications for actin binding. Structure 6: 1419-1431.

Bellanger, J. M., Astier, C., Sardet, C., Ohta, Y., Stossel, T. P. & Debant, A. 2000. The Rac1- and RhoG-specific GEF domain of Trio targets filamin to r emodel cytoskeletal actin. Nat. Cell Biol. 2: 888-892.

Berry, F. B., O'Neill, M. A., Coca-Prados, M. & Walter, M. A. 2005. FOXC1 transcriptional regulatory activity is impaired by PBX1 in a filamin A-mediated manner. Mol. Cell. Biol. 25: 1415-1424.

Bork, P., Holm, L. & Sander, C. 1994. The immunoglobulin fold. Structural classification, sequence patterns and common core. J.Mol.Biol. 242:309-320.

Borrego-Diaz, E., Kerff, F., Lee, S. H., Ferron, F., Li, Y. & Dominguez, R. 2006. Crystal structure of the actin-binding domain of alpha-actinin 1: evaluating two competing actin-binding models. J. Struct. Biol. 155: 230-238.

Bresnick, A. R., Janmey, P. A. & Condeelis, J. 1991. Evidence that a 27-residue sequence is the actin-binding site of ABP-120. J. Biol. Chem. 266: 12989-12993.

Browne, K. A., Johnstone, R. W., Jans, D. A. & Trapani, J. A. 2000. Filamin (280-kDa actin-binding protein) is a caspase substrate and is also cleaved directly by the cytotoxic T lymphocyte protease granzyme B during apoptosis. J. Biol. Chem. 275: 39262-39266.

Calderwood, D. A., Huttenlocher, A., Kiosses, W. B., Rose, D. M., Woodside, D. G., Schwartz, M. A. & Ginsberg, M. H. 2001. Increased filamin binding to beta-integrin cytoplasmic domains inhibits cell migration. Nat. Cell Biol. 3: 1060-1068.

Cho, E. Y., Cho, D. I., Park, J. H., Kurose, H., Caron, M. G. & Kim, K. M. 2007. Roles of protein kinase C and actin-binding protein 280 in the regulation

42

of intracellular trafficking of dopamine D3 receptor. Mol. Endocrinol. 21: 2242-2254.

Clark, A. R., Sawyer, G. M., Robertson, S. P. & Sutherland-Smith, A. J. 2009. Skeletal dysplasias due to filamin A mutations result from a gain-of-function mechanism distinct from allelic neurological disorders. Hum. Mol. Genet. 18: 4791-4800.

D'Addario, M., Arora, P. D., Fan, J., Ganss, B., Ellen, R. P. & McCulloch, C. A. 2001. Cytoprotection against mechanical forces delivered through beta 1 integrins requires induction of filamin A. J. Biol. Chem. 276: 31969-31977.

Dalley, J. W. & Everitt, B. J. 2009. Dopamine receptors in the learning, memory and drug reward circuitry. Semin. Cell Dev. Biol. 20: 403-410.

Donaldson, J. C., Dise, R. S., Ritchie, M. D. & Hanks, S. K. 2002. Nephrocystin-conserved domains involved in targeting to epithelial cell-cell junctions, interaction with filamins, and establishing cell polarity. J. Biol. Chem. 277: 29028-29035.

Dyson, J. M., O'Malley, C. J., Becanovic, J., Munday, A. D., Berndt, M. C., Coghill, I. D., Nandurkar, H. H., Ooms, L. M. & Mitchell, C. A. 2001. The SH2-containing inositol polyphosphate 5-phosphatase, SHIP-2, binds filamin and regulates submembraneous actin. J. Cell Biol. 155: 1065-1079.

Enz, R. & Croci, C. 2003. Different binding motifs in metabotropic glutamate receptor type 7b for filamin A, protein phosphatase 1C, protein interacting with protein kinase C (PICK) 1 and syntenin allow the formation of multimeric protein complexes. Biochem. J. 372: 183-191.

Feng, Y., Chen, M. H., Moskowitz, I. P., Mendonza, A. M., Vidali, L., Nakamura, F., Kwiatkowski, D. J. & Walsh, C. A. 2006. Filamin A (FLNA) is required for cell-cell contact in vascular development and cardiac morphogenesis. Proc. Natl. Acad. Sci. U. S. A. 103: 19836-19841.

Feng, Y. & Walsh, C. A. 2004. The many faces of filamin: a versatile molecular scaffold for cell motility and signalling. Nat. Cell Biol. 6: 1034-1038.

Fox, J. W., Lamperti, E. D., Eksioglu, Y. Z., Hong, S. E., Feng, Y., Graham, D. A., Scheffer, I. E., Dobyns, W. B., Hirsch, B. A., Radtke, R. A., Berkovic, S. F., Huttenlocher, P. R. & Walsh, C. A. 1998. Mutations in filamin 1 prevent migration of cerebral cortical neurons in human periventricular heterotopia. Neuron 21: 1315-1325.

Gahmberg, C. G., Fagerholm, S. C., Nurmi, S. M., Chavakis, T., Marchesan, S. & Gronholm, M. 2009. Regulation of integrin activity and signalling. Biochim. Biophys. Acta 1790: 431-444.

Galkin, V. E., Orlova, A., VanLoock, M. S., Rybakova, I. N., Ervasti, J. M. & Egelman, E. H. 2002. The utrophin actin-binding domain binds F-actin in two different modes: implications for the spectrin superfamily of proteins. J. Cell Biol. 157: 243-251.

Garcia-Alvarez, B., Bobkov, A., Sonnenberg, A. & de Pereda, J. M. 2003. Structural and functional analysis of the actin binding domain of plectin suggests alternative mechanisms for binding to F-actin and integrin beta4. Structure 11: 615-625.

Gehler, S., Baldassarre, M., Lad, Y., Leight, J. L., Wozniak, M. A., Riching, K. M., Eliceiri, K. W., Weaver, V. M., Calderwood, D. A. & Keely, P. J. 2009. Filamin A-beta1 integrin complex tunes epithelial cell response to matrix tension. Mol. Biol. Cell 20: 3224-3238.

Gimona, M., Djinovic-Carugo, K., Kranewitter, W. J. & Winder, S. J. 2002. Functional plasticity of CH domains. FEBS Lett. 513: 98-106.

Gkretsi, V., Zhang, Y., Tu, Y., Chen, K., Stolz, D. B., Yang, Y., Watkins, S. C. & Wu, C. 2005. Physical and functional association of migfilin with cell-cell adhesions. J. Cell. Sci. 118: 697-710.

Glogauer, M., Arora, P., Chou, D., Janmey, P. A., Downey, G. P. & McCulloch, C. A. 1998. The role of actin-binding protein 280 in integrin-dependent mechanoprotection. J. Biol. Chem. 273: 1689-1698.

Gorlin, J. B., Yamin, R., Egan, S., Stewart, M., Stossel, T. P., Kwiatkowski, D. J. & Hartwig, J. H. 1990. Human endothelial actin-binding protein (ABP-280, nonmuscle filamin): a molecular leaf spring. J. Cell Biol. 111: 1089-1105.

Gravante, B., Barbuti, A., Milanesi, R., Zappi, I., Viscomi, C. & DiFrancesco, D. 2004. Interaction of the pacemaker channel HCN1 with filamin A. J. Biol. Chem. 279: 43847-43853.

Grimbert, P., Valanciute, A., Audard, V., Lang, P., Guellaen, G. & Sahali, D. 2004. The Filamin-A is a partner of Tc-mip, a new adapter protein involved in c-maf-dependent Th2 signaling pathway. Mol. Immunol. 40: 1257-1261.

Harburger, D. S., Bouaouina, M. & Calderwood, D. A. 2009. Kindlin-1 and -2 directly bind the C-terminal region of beta integrin cytoplasmic tails and exert integrin-specific activation effects. J. Biol. Chem. 284: 11485-11497.

Hart, A. W., Morgan, J. E., Schneider, J., West, K., McKie, L., Bhattacharya, S., Jackson, I. J. & Cross, S. H. 2006. Cardiac malformations and midline skeletal defects in mice lacking filamin A. Hum. Mol. Genet. 15: 2457-2467.

He, H. J., Kole, S., Kwon, Y. K., Crow, M. T. & Bernier, M. 2003. Interaction of filamin A with the insulin receptor alters insulin-dependent activation of the mitogen-activated protein kinase pathway. J. Biol. Chem. 278: 27096-27104.

Hock, R. S. & Condeelis, J. S. 1987. Isolation of a 240-kilodalton actin-binding protein from Dictyostelium discoideum. J. Biol. Chem. 262: 394-400.

Hynes, R. O. 2002. Integrins: bidirectional, allosteric signaling machines. Cell 110: 673-687.

Ithychanda, S. S., Das, M., Ma, Y. Q., Ding, K., Wang, X., Gupta, S., Wu, C., Plow, E. F. & Qin, J. 2009a. Migfilin, a molecular switch in regulation of integrin activation. J. Biol. Chem. 284: 4713-4722.

Ithychanda, S. S., Hsu, D., Li, H., Yan, L., Liu, D., Das, M., Plow, E. F. & Qin, J. 2009b. Identification and characterization of multiple similar ligand-binding repeats in filamin: implication on filamin-mediated receptor clustering and cross-talk. J. Biol. Chem. 284: 35113-35121.

Kainulainen, T., Pender, A., D'Addario, M., Feng, Y., Lekic, P. & McCulloch, C. A. 2002. Cell death and mechanoprotection by filamin a in connective

44

tissues after challenge by applied tensile forces. J. Biol. Chem. 277: 21998-22009.

Keep, N. H., Winder, S. J., Moores, C. A., Walke, S., Norwood, F. L. & Kendrick-Jones, J. 1999. Crystal structure of the actin-binding region of utrophin reveals a head-to-tail dimer. Structure 7: 1539-1546.

Kiema, T., Lad, Y., Jiang, P., Oxley, C. L., Baldassarre, M., Wegener, K. L., Campbell, I. D., Ylänne, J. & Calderwood, D. A. 2006. The molecular basis of filamin binding to integrins and competition with talin. Mol. Cell 21: 337-347.

Kim, C., Cho, Y., Kang, C. H., Kim, M. G., Lee, H., Cho, E. G. & Park, D. 2005. Filamin is essential for shedding of the transmembrane serine protease, epithin. EMBO Rep. 6: 1045-1051.

Kim, H., Nakamura, F., Lee, W., Hong, C., Perez-Sala, D. & McCulloch, C. A. 2010a. Regulation of cell adhesion to collagen via beta1 integrins is dependent on interactions of filamin A with vimentin and protein kinase C epsilon. Exp. Cell Res. 316: 1829-1844.

Kim, H., Nakamura, F., Lee, W., Shifrin, Y., Arora, P. & McCulloch, C. A. 2010b. Filamin A is required for vimentin-mediated cell adhesion and spreading. Am. J. Physiol. Cell. Physiol. 298: C221-36.

Kim, H., Sengupta, A., Glogauer, M. & McCulloch, C. A. 2008. Filamin A regulates cell spreading and survival via beta1 integrins. Exp. Cell Res. 314: 834-846.

Kim, K. M., Gainetdinov, R. R., Laporte, S. A., Caron, M. G. & Barak, L. S. 2005. G protein-coupled receptor kinase regulates dopamine D3 receptor signaling by modulating the stability of a receptor-filamin-beta-arrestin complex. A case of autoreceptor regulation. J. Biol. Chem. 280: 12774-12780.

Klaile, E., Muller, M. M., Kannicht, C., Singer, B. B. & Lucka, L. 2005. CEACAM1 functionally interacts with filamin A and exerts a dual role in the regulation of cell migration. J. Cell. Sci. 118: 5513-5524.

Krakow, D., Robertson, S. P., King, L. M., Morgan, T., Sebald, E. T., Bertolotto, C., Wachsmann-Hogiu, S., Acuna, D., Shapiro, S. S., Takafuta, T., Aftimos, S., Kim, C. A., Firth, H., Steiner, C. E., Cormier-Daire, V., Superti-Furga, A., Bonafe, L., Graham Jr, J. M., Grix, A., Bacino, C. A., Allanson, J., Bialer, M. G., Lachman, R. S., Rimoin, D. L. & Cohn, D. H. 2004. Mutations in the gene encoding filamin B disrupt vertebral segmentation, joint formation and skeletogenesis. Nat. Genet. 36: 405-410.

Krief, S., Faivre, J. F., Robert, P., Le Douarin, B., Brument-Larignon, N., Lefrere, I., Bouzyk, M. M., Anderson, K. M., Greller, L. D. Tobin, F. L., Souchet, M. & Bril, A. 1999. Identification and characterization of cvHsp. A novel human small stress protein selectively expressed in cardiovascular and insulin-sensitive tissues. J. Biol. Chem. 274: 36592-36600.

Kuhlman, P. A., Hemmings, L. & Critchley, D. R. 1992. The identification and characterisation of an actin-binding site in alpha-actinin by mutagenesis. FEBS Lett. 304: 201-206.

Kyndt, F., Gueffet, J. P., Probst, V., Jaafar, P., Legendre, A., Le Bouffant, F., Toquet, C., Roy, E., McGregor, L., Lynch, S. A., Newbury-Ecob, R., Tran, V., Young, I., Trochu, J.N., Le Marec, H. & Schott, J.J. 2007. Mutations in the gene encoding filamin A as a cause for familial cardiac valvular dystrophy. Circulation 115: 40-49.

Lad, Y., Kiema, T., Jiang, P., Pentikäinen, O. T., Coles, C. H., Campbell, I. D., Calderwood, D. A. & Ylänne, J. 2007. Structure of three tandem filamin domains reveals auto-inhibition of ligand binding. EMBO J. 26: 3993-4004.

Lebart, M. C., Mejean, C., Casanova, D., Audemard, E., Derancourt, J., Roustan, C. & Benyamin, Y. 1994. Characterization of the actin binding site on smooth muscle filamin. J. Biol. Chem. 269: 4279-4284.

Lee, S. H. & Dominguez, R. 2010. Regulation of actin cytoskeleton dynamics in cells. Mol. Cells 29: 311-325.

Li, C., Yu, S., Nakamura, F., Pentikäinen, O. T., Singh, N., Yin, S., Xin, W. & Sy, M. S. 2010. Pro-prion binds filamin A facilitating its interaction with integrin beta1 and contributes to melanomagenesis. J. Biol. Chem.

Li, M., Bermak, J. C., Wang, Z. W. & Zhou, Q. Y. 2000. Modulation of dopamine D(2) receptor signaling by actin-binding protein (ABP-280). Mol. Pharmacol. 57: 446-452.

Li, M., Li, C., Weingarten, P., Bunzow, J. R., Grandy, D. K. & Zhou, Q. Y. 2002. Association of dopamine D(3) receptors with actin-binding protein 280 (ABP-280). Biochem. Pharmacol. 63: 859-863.

Lin, R., Canfield, V. & Levenson, R. 2002. Dominant negative mutants of filamin A block cell surface expression of the D2 dopamine receptor. Pharmacology 66: 173-181.

Lin, R., Karpa, K., Kabbani, N., Goldman-Rakic, P. & Levenson, R. 2001. Dopamine D2 and D3 receptors are linked to the actin cytoskeleton via interaction with filamin A. Proc. Natl. Acad. Sci. U. S. A. 98: 5258-5263.

Liu, J., Taylor, D. W. & Taylor, K. A. 2004. A 3-D reconstruction of smooth muscle alpha-actinin by CryoEm reveals two different conformations at the actin-binding region. J. Mol. Biol. 338: 115-125.

Loo, D. T., Kanner, S. B. & Aruffo, A. 1998. Filamin binds to the cytoplasmic domain of the beta1-integrin. Identification of amino acids responsible for this interaction. J. Biol. Chem. 273: 23304-23312.

Loy, C. J., Sim, K. S. & Yong, E. L. 2003. Filamin-A fragment localizes to the nucleus to regulate androgen receptor and coactivator functions. Proc. Natl. Acad. Sci. U. S. A. 100: 4562-4567.

Ma, Y. Q., Qin, J., Wu, C. & Plow, E. F. 2008. Kindlin-2 (Mig-2): a co-activator of beta3 integrins. J. Cell Biol. 181: 439-446.

Maceyka, M., Alvarez, S. E., Milstien, S. & Spiegel, S. 2008. Filamin A links sphingosine kinase 1 and sphingosine-1-phosphate receptor 1 at lamellipodia to orchestrate cell migration. Mol. Cell. Biol. 28: 5687-5697.

Marti, A., Luo, Z., Cunningham, C., Ohta, Y., Hartwig, J., Stossel, T. P., Kyriakis, J. M. & Avruch, J. 1997. Actin-binding protein-280 binds the stress-activated protein kinase (SAPK) activator SEK-1 and is required for tumor

necrosis factor-alpha activation of SAPK in melanoma cells. J. Biol. Chem. 272: 2620-2628.

Missale, C., Nash, S. R., Robinson, S. W., Jaber, M. & Caron, M. G. 1998. Dopamine receptors: from structure to function. Physiol. Rev. 78: 189-225.

Nagano, T., Yoneda, T., Hatanaka, Y., Kubota, C., Murakami, F. & Sato, M. 2002. Filamin A-interacting protein (FILIP) regulates cortical cell migration out of the ventricular zone. Nat. Cell Biol. 4: 495-501.

Nakagawa, K. Sugahara, M., Yamasaki, T., Kajiho, H., Takahashi, S., Hirayama, J., Minami, Y., Ohta, Y., Watanabe, T., Hata, Y., Katada, T. & Nishina, H. 2010. Filamin associates with stress signalling kinases MKK7 and MKK4 and regulates JNK activation. Biochem. J. 427: 237-245.

Nakamura, F., Hartwig, J. H., Stossel, T. P. & Szymanski, P. T. 2005. Ca2+ and calmodulin regulate the binding of filamin A to actin filaments. J. Biol. Chem. 280: 32426-32433.

Nakamura, F., Heikkinen, O., Pentikäinen, O. T., Osborn, T. M., Kasza, K. E., Weitz, D. A., Kupiainen, O., Permi, P., Kilpeläinen, I., Ylänne, J., Hartwig J. H. & Stossel T. P. 2009. Molecular basis of filamin A-FilGAP interaction and its impairment in congenital disorders associated with filamin A mutations. PLoS One 4: e4928.

Nakamura, F., Osborn, T. M., Hartemink, C. A., Hartwig, J. H. & Stossel, T. P. 2007. Structural basis of filamin A functions. J. Cell Biol. 179: 1011-1025.

Nakamura, F., Pudas, R., Heikkinen, O., Permi, P., Kilpeläinen, I., Munday, A. D., Hartwig, J. H., Stossel, T. P. & Ylänne, J. 2006. The structure of the GPIb-filamin A complex. Blood 107: 1925-1932.

Nikki, M., Meriläinen, J. & Lehto, V. P. 2002. FAP52 regulates actin organization via binding to filamin. J. Biol. Chem. 277: 11432-11440.

Nishida, N., Xie, C., Shimaoka, M., Cheng, Y., Walz, T. & Springer, T. A. 2006. Activation of leukocyte beta2 integrins by conversion from bent to extended conformations. Immunity 25: 583-594.

Ohta, Y., Hartwig, J. H. & Stossel, T. P. 2006. FilGAP, a Rho- and ROCK-regulated GAP for Rac binds filamin A to control actin remodelling. Nat. Cell Biol. 8: 803-814.

Ohta, Y., Suzuki, N., Nakamura, S., Hartwig, J. H. & Stossel, T. P. 1999. The small GTPase RalA targets filamin to induce filopodia. Proc. Natl. Acad. Sci. U. S. A. 96: 2122-2128.

Onoprishvili, I., Andria, M. L., Kramer, H. K., Ancevska-Taneva, N., Hiller, J. M. & Simon, E. J. 2003. Interaction between the mu opioid receptor and filamin A is involved in receptor regulation and trafficking. Mol. Pharmacol. 64: 1092-1100.

Ott, I., Fischer, E. G., Miyagi, Y., Mueller, B. M. & Ruf, W. 1998. A role for tissue factor in cell adhesion and migration mediated by interaction with actin-binding protein 280. J. Cell Biol. 140: 1241-1253.

Ozanne, D. M., Brady, M. E., Cook, S., Gaughan, L., Neal, D. E. & Robson, C. N. 2000. &rogen receptor nuclear translocation is facilitated by the f-actin cross-linking protein filamin. Mol. Endocrinol. 14: 1618-1626.

Pentikäinen, U. & Ylänne, J. 2009. The regulation mechanism for the auto-inhibition of binding of human filamin a to integrin. J Mol Biol 393: 644-657

Petrecca, K., Miller, D. M. & Shrier, A. 2000. Localization and enhanced current density of the Kv4.2 potassium channel by interaction with the actin-binding protein filamin. J. Neurosci. 20: 8736-8744.

Playford, M. P., Nurminen, E., Pentikäinen, O. T., Milgram, S. L., Hartwig, J. H., Stossel, T. P. & Nakamura, F. 2010. Cystic fibrosis transmembrane conductance regulator interacts with multiple immunoglobulin domains of filamin A. J. Biol. Chem. 285: 17156-17165.

Popowicz, G. M., Muller, R., Noegel, A. A., Schleicher, M., Huber, R. & Holak, T. A. 2004. Molecular structure of the rod domain of dictyostelium filamin. J. Mol. Biol. 342: 1637-1646.

Pudas, R., Kiema, T. R., Butler, P. J., Stewart, M. & Ylänne, J. 2005. Structural basis for vertebrate filamin dimerization. Structure 13: 111-119.

Revenu, C., Athman, R., Robine, S. & Louvard, D. 2004. The co-workers of actin filaments: from cell structures to signals. Nat. Rev. Mol. Cell Biol. 5: 635-646.

Robertson, S. P. 2007. Otopalatodigital syndrome spectrum disorders: otopalatodigital syndrome types 1 and 2, frontometaphyseal dysplasia and Melnick-Needles syndrome. Eur. J. Hum. Genet. 15: 3-9.

Robertson, S. P., Twigg, S. R., Sutherland-Smith, A. J., Biancalana, V., Gorlin, R. J., Horn, D., Kenwrick, S. J., Kim, C. A., Morava, E. Newbury-Ecob, R., Orstavik, K. H., Quarrell, O. W., Schwartz, C. E., Shears, D. J. Suri, M., Kendrick-Jones, J., Wilkie, A. O. & OPD-spectrum Disorders Clinical Collaborative Group. 2003. Localized mutations in the gene encoding the cytoskeletal protein filamin A cause diverse malformations in humans. Nat. Genet. 33: 487-491.

Sampson, L. J., Leyland, M. L. & Dart, C. 2003. Direct interaction between the actin-binding protein filamin-A and the inwardly rectifying potassium channel, Kir2.1. J. Biol. Chem. 278: 41988-41997.

Sasaki, A., Masuda, Y., Ohta, Y., Ikeda, K. & Watanabe, K. 2001. Filamin associates with Smads and regulates transforming growth factor-beta signaling. J. Biol. Chem. 276: 17871-17877.

Sawyer, G. M., Clark, A. R., Robertson, S. P. & Sutherland-Smith, A. J. 2009. Disease-associated substitutions in the filamin B actin binding domain confer enhanced actin binding affinity in the absence of major structural disturbance: Insights from the crystal structures of filamin B actin binding domains. J. Mol. Biol. 390: 1030-1047.

Seck, T., Baron, R. & Horne, W. C. 2003. Binding of filamin to the C-terminal tail of the calcitonin receptor controls recycling. J. Biol. Chem. 278: 10408-10416.

Seo, M. D., Seok, S. H., Im, H., Kwon, A. R., Lee, S. J., Kim, H. R., Cho, Y., Park, D. & Lee, B. J. 2009. Crystal structure of the dimerization domain of human filamin A. Proteins 75: 258-263.

48

Sheen, V. L., Dixon, P. H., Fox, J. W., Hong, S. E., Kinton, L., Sisodiya, S. M., Duncan, J. S., Dubeau, F., Scheffer, I. E., Schachter, S. C., Wilner, A., Henchy, R., Crino, P., Kamuro, K., DiMario, F., Berg, M., Kuzniecky, R., Cole, A. J., Bromfield, E., Biber, M., Schomer, D., Wheless, J., Silver, K., Mochida, G. H., Berkovic, S. F., Andermann, F., Andermann, E., Dobyns, W. B., Wood, N. W. & Walsh, C. A. 2001. Mutations in the X-linked filamin 1 gene cause periventricular nodular heterotopia in males as well as in females. Hum. Mol. Genet. 10: 1775-1783.

Shifrin, Y., Arora, P. D., Ohta, Y., Calderwood, D. A. & McCulloch, C. A. 2009. The role of FilGAP-filamin A interactions in mechanoprotection. Mol. Biol. Cell 20: 1269-1279.

Sjekloca, L., Pudas, R., Sjöblom, B., Konarev, P., Carugo, O., Rybin, V., Kiema, T. R., Svergun, D., Ylänne, J. & Djinovic-Carugo, K. 2007. Crystal structure of human filamin C domain 23 and small angle scattering model for filamin C 23-24 dimer. J. Mol. Biol. 368: 1011-1023.

Smith, L., Page, R. C., Xu, Z., Kohli, E., Litman, P., Nix, J. C., Ithychanda, S. S., Liu, J., Qin, J., Misra, S. & Liedtke, C. M. 2010. Biochemical basis of the interaction between cystic fibrosis transmembrane conductance regulator and immunoglobulin-like repeats of filamin. J. Biol. Chem. 285: 17166-17176.

Sokol, N. S. & Cooley, L. 1999. Drosophila filamin encoded by the cheerio locus is a component of ovarian ring canals. Curr. Biol. 9: 1221-1230.

Stahlhut, M. & van Deurs, B. 2000. Identification of filamin as a novel ligand for caveolin-1: evidence for the organization of caveolin-1-associated membrane domains by the actin cytoskeleton. Mol. Biol. Cell 11: 325-337.

Stokroos, I., Kalicharan, D., Van der Want, J. J. L. & Jongebloed, W.L. 1998. A comparative study of thin coatings of Au/Pd, Pt and Cr produced by magnetron sputtering for FE-SEM. J. Microsc. 189: 79-79-89

Stossel, T. P., Condeelis, J., Cooley, L., Hartwig, J. H., Noegel, A., Schleicher, M. & Shapiro, S. S. 2001. Filamins as integrators of cell mechanics and signalling. Nat. Rev. Mol. Cell Biol. 2: 138-145.

Svergun, D. I., Petoukhov, M. V. & Koch, M. H. 2001. Determination of domain structure of proteins from X-ray solution scattering. Biophys. J. 80: 2946-2953.

Takabayashi, T. M., Xie, J., Takeuchi, S., Kawasaki, M., Yagi, H., Okamoto, M., Tariqur, R. M., Malik, F., Kuroda, K., Kubota, C., Fujieda, S., Nagano, T. & Sato, M. 2010. LL5beta directs the translocation of filamin A and SHIP2 to sites of phosphatidylinositol 3,4,5-triphosphate (PtdIns(3,4,5)P3) accumulation, and PtdIns(3,4,5)P3 localization is mutually modified by co-recruited SHIP2. J. Biol. Chem. 285: 16155-16165.

Takafuta, T., Saeki, M., Fujimoto, T. T., Fujimura, K. & Shapiro, S. S. 2003. A new member of the LIM protein family binds to filamin B and localizes at stress fibers. J. Biol. Chem. 278: 12175-12181.

Takafuta, T., Wu, G., Murphy, G. F. & Shapiro, S. S. 1998. Human beta-filamin is a new protein that interacts with the cytoplasmic tail of glycoprotein Ibalpha. J. Biol. Chem. 273: 17531-17538.

Takagi, J., Petre, B. M., Walz, T. & Springer, T. A. 2002. Global conformational rearrangements in integrin extracellular domains in outside-in and inside-out signaling. Cell 110: 599-511.

Takala, H., Nurminen, E., Nurmi, S. M., Aatonen, M., Strandin, T., Takatalo, M., Kiema, T., Gahmberg, C. G., Ylänne, J. & Fagerholm, S. C. 2008. Beta2 integrin phosphorylation on Thr758 acts as a molecular switch to regulate 14-3-3 and filamin binding. Blood 112: 1853-1862.

Thompson, T. G., Chan, Y. M., Hack, A. A., Brosius, M., Rajala, M., Lidov, H. G., McNally, E. M., Watkins, S. & Kunkel, L. M. 2000. Filamin 2 (FLN2): A muscle-specific sarcoglycan interacting protein. J. Cell Biol. 148: 115-126.

Tigges, U., Koch, B., Wissing, J., Jockusch, B. M. & Ziegler, W. H. 2003. The F-actin cross-linking and focal adhesion protein filamin A is a ligand and in vivo substrate for protein kinase C alpha. J. Biol. Chem. 278: 23561-23569.

Tu, Y., Wu, S., Shi, X., Chen, K. & Wu, C. 2003. Migfilin and Mig-2 link focal adhesions to filamin and the actin cytoskeleton and function in cell shape modulation. Cell 113: 37-47.

Ueda, K., Ohta, Y. & Hosoya, H. 2003. The carboxy-terminal pleckstrin homology domain of ROCK interacts with filamin-A. Biochem. Biophys. Res. Commun. 301: 886-890.

Wepf, R., Amrein, M., Burkli, U. & Gross, H. 1991. Platinum/iridium/carbon: a high-resolution shadowing material for TEM, STM and SEM of biological macromolecular structures. J.Microsc. 163:51-64.

Vadlamudi, R. K., Li, F., Adam, L., Nguyen, D., Ohta, Y., Stossel, T. P. & Kumar, R. 2002. Filamin is essential in actin cytoskeletal assembly mediated by p21-activated kinase 1. Nat. Cell Biol. 4: 681-690.

Vallone, D., Picetti, R. & Borrelli, E. 2000. Structure and function of dopamine receptors. Neurosci. Biobehav. Rev. 24: 125-132.

van der Flier, A. & Sonnenberg, A. 2001. Structural and functional aspects of filamins. Biochim. Biophys. Acta 1538: 99-117.

Vargas, M., Sansonetti, P. & Guillen, N. 1996. Identification and cellular localization of the actin-binding protein ABP-120 from Entamoeba histolytica. Mol. Microbiol. 22: 849-857.

Vorgerd, M., van der Ven, P. F., Bruchertseifer, V., Lowe, T., Kley, R., Schroder, R. A., Lochmuller, H., Himmel, M., Koehler, K., Furst D. O. & Huebner, A. 2005. A mutation in the dimerization domain of filamin c causes a novel type of autosomal dominant myofibrillar myopathy. Am. J. Hum. Genet. 7 7: 297-304.

Xiong, J. P., Stehle, T., Diefenbach, B., Zhang, R., Dunker, R., Scott, D. L., Joachimiak, A., Goodman, S. L. & Arnaout, M. A. 2001. Crystal structure of the extracellular segment of integrin alpha Vbeta3. Science 294: 339-345.

Yoshida, N., Ogata, T., Tanabe, K., Li, S., Nakazato, M., Kohu, K., Takafuta, T., Shapiro, S., Ohta, Y., Satake, M. & Watanabe, T. 2005. Filamin A-bound

PEBP2beta/CBFbeta is retained in the cytoplasm and prevented from functioning as a partner of the Runx1 transcription factor. Mol. Cell. Biol. 25: 1003-1012.

Yuan, Y. & Shen, Z. 2001. Interaction with BRCA2 suggests a role for filamin-1 (hsFLNa) in DNA damage response. J. Biol. Chem. 276: 48318-48324.

Zhang, W., Han, S. W., McKeel, D. W., Goate, A. & Wu, J. Y. 1998. Interaction of presenilins with the filamin family of actin-binding proteins. J. Neurosci. 18: 914-922.

Zhang, Y., Tu, Y., Gkretsi, V. & Wu, C. 2006. Migfilin interacts with vasodilator-stimulated phosphoprotein (VASP) and regulates VASP localization to cell-matrix adhesions and migration. J. Biol. Chem. 281: 12397-12407.

Zhou, A. X., Hartwig, J. H. & Akyurek, L. M. 2010. Filamins in cell signaling, transcription and organ development. Trends Cell Biol. 20: 113-123.